Effect of gas-transfer velocity parameterization choice on CO_2 air-sea fluxes in the North Atlantic and the European Arctic

Iwona Wrobel[1] and Jacek Piskozub[1]

[1] Institute of Oceanology, Polish Academy of Sciences, Sopot, Poland

Correspondence to: I. Wróbel (iwrobel@iopan.gda.pl)

Abstract

The oceanic sink of carbon dioxide (CO_2) is an important part of the global carbon budget. Understanding uncertainties in the calculation of this net flux into the ocean is crucial for climate research. One of the sources of the uncertainty within this calculation is the parameterization chosen for the CO_2 gas transfer velocity. We used a recently developed software toolbox, called the FluxEngine, to estimate the monthly net carbon air-sea flux for the extratropical North Atlantic, the European Arctic, and globally using several published quadratic and cubic wind speed parameterizations of the gas transfer velocity. The aim of the study is to constrain the uncertainty caused by the choice of parameterization in the North Atlantic. This region is considered a large oceanic sink of CO_2, and it is also a region often characterised by strong winds but with good in situ measurement coverage. We show that this uncertainty is smaller in the North Atlantic and the Arctic than globally. It is as little as 5% in the North Atlantic and 4% in the European Arctic, in comparison to 9% for the global ocean when restricted to functions with quadratic wind dependence. Whereas this uncertainty becomes 46%, 44% and 65% respectively if you consider all of the parameterizations studied. We propose that this smaller uncertainty is caused by a combination of higher than global average wind speeds in the North Atlantic and lack of any seasonal changes in the direction of the flux direction within most of the region. We also compare the impact of using two different in situ $p\text{CO}_2$ datasets (Takahashi and SOCAT) within the flux calculation. Differences in these $p\text{CO}_2$ data in turn cause differences in the annual net flux values of 8% in the North Atlantic and 19% in the European Arctic. The seasonal flux in the Arctic computed from two climatology data sets are opposite to one another, possibly due to insufficient spatial and temporal data coverage, especially in winter.

1. Introduction

The region of extratropical North Atlantic, including the European Arctic, is a region responsible for the formation of deep ocean waters (see Talley (2013) for a recent review). This process, part of the global overturning circulation, makes the area a large sink of CO_2 (Takahashi et al., 2002; Takahashi et al., 2009; Landschützer et al., 2014; Le Quéré et al., 2015). Therefore, there is a widespread interest in tracking the changes in the North Atlantic net carbon fluxes, especially as models appear to predict a decrease in the sink volume later this century (Halloran et al., 2015).

The trend and variations in the North Atlantic CO_2 sink has been intensively studied since observations have shown it appears to be decreasing (Lefèvre et al., 2004). This decrease on inter-annual time scales has been confirmed by further studies (Schuster and Watson, 2007) and this trend has continued in recent years North of 40º N (Landschützer et al., 2013). It is not certain how many of these changes are the result of long-term changes, decadal changes in atmospheric forcing, namely the North Atlantic Oscillation (Gonzalez-Davila et al., 2007; Thomas et al., 2008; Gruber 2009; Watson et al., 2009) or changes in meridional overturning circulations (Perez et al., 2013).

Recent assessments of the Atlantic and Arctic net sea–air CO_2 fluxes (Schuster et al., 2013) and the global ocean net carbon uptake (Wanninkhof et al., 2013) show that the cause is still unknown.

To study the rate of the ocean CO_2 sink and especially its long-term trend, one needs to first constrain the total uncertainty in the flux calculation. Sources of uncertainty include sampling coverage, the method of data interpolation, in-water fugacity data quality, the method used for normalization of fugacity data to a reference year in a world of ever increasing atmospheric CO_2 partial pressure and the choice of gas transfer velocity *k* parameterization (Landschützer et al., 2014; Woolf et al., 2015a, 2015b). It has also been identified that the choice of the wind data product provides an additional source of uncertainty (Gregg et al., 2015). In this work we have chosen to analyze various empirical wind driven gas transfer parameterizations. Although the North Atlantic is one of the regions of the world ocean best covered by CO_2 fugacity measurements (Watson et al., 2011), the Arctic seas coverage is much poorer, especially in winter (Schuster et al., 2013).

One of the factors influencing the value of the calculated net air-sea gas flux is the choice of the formula for the gas transfer velocity. Within the literature there are many different parameterizations to choose from, but most depend on a cubic or quadratic wind speed relationship. The choice of parameterization is not trivial as indicated by the name of an international meeting that focussed on the topic implies ("*k* conundrum" workshop, COST-735 Action organized meeting in Norwich, February 2008). The conclusions from this meeting have been incorporated into a recent review book chapter (Garbe et al., 2014). This paper concentrates on quantifying the uncertainty caused by the choice of the gas transfer velocity parameterization in the North Atlantic and the European Arctic. These regions were chosen as they are the areas for which many of the parameterization was originally derived. They are also regions with wind distributions skewed towards higher winds (in comparison to the global average) enabling the effect of stronger winds on the net flux calculations to be investigated through using published gas transfer velocity formulas.

2. Methods

2.1 Datasets

We calculated net air-sea CO_2 fluxes using a set of software processing tools called the 'FluxEngine' (Shutler et al., 2016), which were created within European Space Agency funded OceanFlux Greenhouse Gases project (http://www.oceanflux-ghg.org). All gas flux calculations were performed using the FluxEngine software. The tools were developed to provide the community with a verified and consistent toolbox and to encourage the use of satellite Earth Observation (EO) data for studying air-sea fluxes. The toolbox source code can be downloaded or alternatively there is a version that can be run through a web interface. Within the online web interface, a suite of reanalysis data products, *in situ* and model data are available as input to the toolbox. These data are freely available for the scientific community to use. The FluxEngine allows you to select several different air-sea flux parameterizations, as well as input data, allowing the generation of the monthly global gridded net air-sea flux products with 1º x 1º spatial resolution. The output consists of twelve NetCDF files (one file per month). Some Monthly composite file includes the mean (first order moment), median, standard deviation and the second, third and fourth order moments. There is also information (meta data) about origin of data inputs. Users can choose from all of the data available on the web portal (example monthly EO input data include: rain intensity, wind speed and direction, % of sea ice cover from monthly model data, ECMWF air pressure, whitecapping (Goddijn-Murphy et al., 2011), two options for monthly climatology of pCO_2, SST, salinity). The user then needs to choose the different components and structure of the net air-sea gas flux calculation and choose the transfer velocity parametrization.

For the calculations, we used pCO_2 and salinity values from Takahashi et al. (2009) climatology which is based on more than 3 million measurements of surface water pCO_2 in open-ocean environments during non El Nino conditions. For some calculations we used, as an alternative, Surface Ocean CO_2 Atlas (SOCAT) ver. 1.5 and 2.0 (Sabine et al., 2013; Pfeil et al., 2013; Bakker et al., 2014) pCO_2 and associated SST data. SOCAT is a community driven dataset containing respectively 6.3 and 10.1 million surface water CO_2 fugacity values with a global coverage. The SOCAT databases have been re-analysed and then converted to climatologies using the methodology described in Goddijn-Murphy et al. (2015). All the climatologies were calculated for year 2010 within the FluxEngine toolset. The SSTfnd values were taken from Operational Sea Surface Temperature and Sea Ice Analysis (OSTIA) (Donlon et al., 2011), and in the case of SOCAT database, while SST skin data that we use come from ARC/(A)ATSR Global Monthly Sea Surface dataset (Merchant et al., 2012). Both data sets have been preprocessed in the same way for use with the FluxEngine (Shutler et al., 2016).

We used Earth Observation (EO) wind speed and sea roughness (σ_0 in Ku band from GlobWave L2P products) data obtained from the European Space Agency (ESA). The GlobWave satellite products give a "uniform" set of along track satellite wave data from all available Altimeters (spanning multiple space agencies) and from ESA Synthetic Aperture Radar (SAR) data. GlobWave Project is an initiative funded by ESA and subsidised by CNES. The aim of the project is to improve the uptake of satellite-derived wind-wave and swell data by the scientific, operational and commercial user communities. This has been achieved by providing a uniform, harmonized, quality controlled, multi-sensor set of satellite wave data. Wave data is collected from both altimeters (ERS-1, ERS-2, ENVISAT, Topex/POSEIDON, Jason-1, Jason-2, CryoSAT, GEOSAT and GEOSAT Follow On) and from ESA Synthetic Aperture Radar (SAR) missions, namely ERS-1, ERS-2 and ENVISAT. All data come in netCDF-3 format.

All analyses were performed using global data within the FluxEngine software. From the gridded product (1° x 1°) we extracted the extratropical North Atlantic (north of 30º N), and its subset, the European Arctic (north of 64º N). For comparison, we also calculated fluxes in the Southern Ocean (south of 40º S). Hereafter we follow the convention of that sources of CO_2 (upward ocean-to-atmosphere gas fluxes) are positive and sinks (downward atmosphere-to-ocean gas fluxes) are negative. We give all results of net CO_2 fluxes in the SI unit of Pg (which is numerically identical to Gt).

2.2. *k* parameterizations

The flux of CO_2 at the interface of air and the sea is controlled by wind speed, sea state, sea surface temperature (SST) and other factors. We estimate the net air-sea flux of CO_2 (F, mg C m^{-2} day^{-1}) as the product of gas transfer velocity (k, ms^{-1}) and also the difference in CO_2 concentration (gm^{-3}) within the sea water and its interface with the air (Land et al., 2013). The concentration of CO_2 in sea water is the product of its solubility (α, gm^{-3} μatm^{-1}) and its fugacity (fCO_2, μatm). Solubility is in turn, a function of salinity and temperature. Hence F is defined as:

$$F = k\,(\alpha_W\, fCO_{2W} - \alpha_S\, fCO_{2A}) \qquad (1)$$

where the subscripts denote values in water (W) and the air-sea interface (S) and in the air (A). We can exchange fugacity to the partial pressure (their values differ by <0.5 % over the temperature range considered) (McGillis et al., 2001). So equation (1) now becomes:

$$F = k\,(\alpha_W\, pCO_{2W} - \alpha_S\, pCO_{2A}) \qquad (2)$$

One can also ignore the differences between the two solubilites, and just use the waterside solubility α_W. Equation (2) will be represented then as:

$$F = k\,\alpha_W\,(pCO_{2W} - pCO_{2A}) \qquad (3)$$

This formulation is often referred to as the 'bulk parametrization'.

In this work we chose to analyze the air-sea gas fluxes using five different gas transfer parameterizations (*k*). All of them are wind speed parameterizations, but differ in the formula used:

$$k = \sqrt{(660.0/ Sc_{skin})} * (0.212\, U_{10}^2 + 0.318\, U_{10}) \qquad (4)$$

(Nightingale et al., 2000),

$$k = \sqrt{(660.0/ Sc_{skin})} * 0.254\, U_{10}^2 \qquad (5)$$

(Ho et al., 2006),

$$k = \sqrt{(660.0/ Sc_{skin})} * 0.0283\, U_{10}^3 \qquad (6)$$

(Wanninkhof and McGillis, 1999),

$$k = \sqrt{(660.0/ Sc_{skin})} * 0.251\, U_{10}^2 \qquad (7)$$

(Wanninkhof, 2014),

$$k = \sqrt{(660.0/ Sc_{skin})} * (3.3 + 0.026\, U_{10}^3) \qquad (8)$$

(McGillis et al., 2001),

where the subscripts are Schmidt numbers at the skin surface (Sc_{skin}), a function of SST ([= (kinematic viscosity of water)/(diffusion coefficient of CO_2 in water)]), 660.0 is the Schmidt number for carbon dioxide at 20 ºC temperature in seawater, U_{10} is the wind speed 10 m above the sea surface.

In addition to the purely wind driven parameterizations, we have used the combined Goddijn-Murphy et al. (2012) and Fangohr and Woolf (2007) parametrization, which was developed as a test algorithm within of OceanFlux GHG Evolution project and it is provided as an option in the FluxEngine toolbox. This parameterization separates contributions from direct- and bubble-mediated gas transfer as suggested by Woolf (2005). Its purpose is to enable a separate evaluation of the effect of the two processes on air-sea gas fluxes and it is an algorithm that has yet to be calibrated (one of the aims of the ongoing OceanFlux Evolution project is to develop a calibration for this algorithm). We used two versions of this parameterization: wind driven direct transfer (using the U10 wind fields) and radar backscatter driven direct transfer (using mean wave square slope) as described in Goddijn-Murphy et al. (2012).

3. Results

Using the FluxEngine software, we have produced net CO_2 global monthly gridded air-sea fluxes and from these we have extracted the values for the two study regions, the extratropical North Atlantic and separately for its subset, the European Arctic seas. Figure 1 shows maps of the monthly mean CO_2 air-sea fluxes for the North Atlantic, calculated with Nightingale et al. (2000) (hereafter called N2000) *k* parameterization and the Takahashi et al. (2009) climatology for the whole year and for each season. The area, as a whole, is a sink of CO_2 but even the seasonal maps show that some regions close to North Atlantic Drift and East Greenland Current are net sources. The seasonal maps show even more variability. For example, the areas close to the North Atlantic Drift And East

Greenland current are sinks of CO_2 in the summer (likely due to the growth of phytoplankton) while the southern most areas of the region become CO_2 sources in summer and autumn (which is likely to be due to the effect of sea-water temperature changes). Much of this variability is caused by changes of the surface water pCO_2 average values, shown in Figure 2 for the whole year and for each season (and variability in atmospheric CO_2 partial pressure, not shown). However, the flux is proportional to the product of ΔpCO_2 and k. In most parameterizations k is a function of wind speed (eqs. 4-8). The mean wind speed U_{10} for the whole year and each season are shown in Figure 3. The wind speeds in the North Atlantic are higher than the mean value in the world ocean, with mean values higher than 10 m s^{-1} in many regions of the study area in all seasons except for the summer (with highest values in winter). This is important because the air-sea flux depends not only on average wind speed but also on its distribution (see also the Discussion). This effect is especially visible between formulas with different powers of U_{10}. Figure 4 shows the difference in the air-sea fluxes calculated using two example parameterizations: one proportional to U_{10}^3 (eq. 6) and one to U_{10}^2 (eq. 7), namely Wanninkhof and McGillis (1999) and Wanninkhof (2014). It can be seen that the "cubic" function results in higher absolute air-sea flux values when compared to the "quadratic" function in the regions of high winds, and lower absolute air-sea flux values in weaker winds.

Figure 5 shows the monthly values of CO_2 air-sea fluxes for the five parameterizations (eq. 4-8) for the North Atlantic and the European Arctic. The regions are sinks of CO_2 in every month, although August is close to neutral for the North Atlantic. The results using cubic parameterizations (eqs. 6 and 8) are higher in absolute values, respectively by up to 30% for Wanninkhof and McGillis (1999) and 55% for McGillis (2001), in comparison to the "quadratic" of N2000 (eq. 4). The other two "quadratic" parameterizations (eqs. 5 and 7) resulted in fluxes within 5% of N2000. Annual net fluxes for the North Atlantic and the European Arctic and global (included for comparison) are shown in Table 1. In addition to the five parameterizations, the figure presents results for both of the OceanFlux GHG Evolution formulas (using wind and radar backscatter data). The mean and standard deviations of the parametrization ensemble are shown as grey vertical lines. The standard deviation in global fluxes is similar to previous estimates (Sweeney et al., 2007, Landschützer et al., 2014) but they cannot be directly compared due to different parameterization choices and methodologies. The results show that the annual North Atlantic net air-sea CO_2 sink, depending on the formula used, varies from -0.38 Pg C for N2000 to -0.56 Pg C for McGillis et al. (2001). In the case of global net air-sea CO_2 sink the values are, respectively, -1.30 Pg C and -2.15 Pg C. Table 1 as well as Figure 6 show the same data "normalized" to the N2000 data (divided by value), this allows us to visualize the relative differences. In the case of the North Atlantic using the "quadratic" Wanninkhof (2014) and Ho et al. (2006) parameterizations results in a net air-sea flux that is 4% and 5% higher in absolute value than the equivalent N2000 result, while the "cubic" Wanninkhof and McGillis (1999) and McGillis et al. (2001) results in values that are up to 28% and 44%. The respective values for the Arctic are 3%, 4% for quadratic as well as 28% and 44% for cubic functions. In the case of global net air-sea CO_2 flux the equivalent values are 8% and 9% higher than the N2000 result for the quadratic functions as well as 33% and 65% for cubic ones. The OceanFlux GHG parameterization results in net air-sea CO_2 fluxes that are 38% and 47% higher for North Atlantic than the N2000 result (for the backscatter and wind driven versions respectively). The spread of the Arctic values was lower than the Atlantic ones (see Table 1). On the other hand, the values for the South Ocean were slightly higher than for North Atlantic but lower than the global ones, with the exception of the OceanFlux GHG parameterizations. In the case of global values the values were, 44% and 52% respectively.

All the above results used the Takahashi (2009) pCO_2 climatology. For comparison we have also calculated the air-sea fluxes using the re-analysed SOCAT version 1.5 and 2.0 data (Goddijn-Murphy et al., 2015). Figure 7 shows the results using the N2000 k parameterization for all three of the climatologies. In the case of the North Atlantic study area, although the monthly values show large differences (using both SOCAT datasets results in a larger sink in summer and smaller in winter compare to Takahashi), the annual values are similar: -0.38 Pg C for both Takahashi and SOCAT v.1.5 and -0.41 Pg C for SOCAT v. 2.0. In the case of the European Arctic the situation is very different, with Takahashi and SOCAT dataset derived climatologies resulting in inverse seasonal variability but with annual net air-sea CO_2 flux results that are similar: -0.102 Pg C for Takahashi, -0.085 Pg C for SOCAT v. 1.5 and -0.088 Pg C for SOCAT v. 2.0.

4. Discussion

Our results show that using the three "quadratic" parameterizations (Nightingale et al., 2000; Ho et al., 2006 and Wanninkhof 2014) results in air-sea flux values that are within 5% of each other in the case of the North Atlantic. This discrepancy is smaller than the 9% difference identified for the global case (Fig. 6). This result confirms that at present, these different parameterizations are interchangeable for the North Atlantic as this variation is within the experimental uncertainty (Nightingale, 2015). The three parameterizations were derived using different methods and data from different regions, namely passive tracers and dual-trace experiments in the North Sea in the case of Nightingale et al. (2000), dual tracers in the Southern Ocean in the case of Ho et al. (2006) and global ocean ^{14}C inventories in the case of Wanninkhof (2014). The differences between these and the quadratic parameterization are large and although the quadratic functions are supported by several lines of evidence (see Garbe et. al., 2014 for discussion). Therefore, it is important to notice that a choice of one of the available cubic functions may lead to net air-sea CO_2 fluxes that are considerably larger in absolute values, by up to 33% in the North Atlantic and more than 50% globally.

The above results imply smaller relative differences between the parameterizations in the North Atlantic than globally. This is interesting because the North Atlantic is the region of strong winds and over most of its area there are no seasonal change in the air-sea flux direction (Fig. 1). For example in the South Atlantic annual mean of wind speed is within 8.48 m s^{-1} (Takahashi et al., 2009) and sink of CO_2 (south of 45°) decrease significantly after 1990 with increasing wind speeds what can influence higher concentration of pCO_2 in surface water due to enhance vertical mixing of deep waters and biological activity. (Le Quèrè et al., 2007). Takahashi et al. (2009) also indicate that the flux difference in the Southern Ocean are very strong dependence to the choice of the gas parameterizations and wind speed. This is more surprising, for North Atlantic, given that at least some of the older parameterizations were developed using a smaller range of winds than can exist in the North Atlantic. After analysis of this unexpected fact, using the formula multiplied by the different wind distribution, we have found two reasons for this. First, when comparing quadratic and cubic parameterizations (Fig. 8), cubic parameterization imply higher air-sea fluxes for high winds, while quadratic one for weaker winds. This difference can be presented in arithmetic terms. Let us assume two functions of wind speed U, $F_1(U)$ quadratic and $F_2(U)$ cubic:

$$F_1(U) = a\,U^2, \qquad (9)$$

$$F_2(U) = b\,U^3. \qquad (10)$$

The difference between the two functions ΔF is equal to:

$$\Delta F = F_2 - F_1 = b\,U^3 - a\,U^2 = b\,U^2\,(U - a\,b^{-1}) = b\,U^2\,(U - U_x) \qquad (11)$$

where $U_x = a\,b^{-1}$. The difference is positive for wind speeds greater than U_x and negative for winds less U_x. U_x is the value of wind speed for which the two functions intersect. In the case of equations (6) and (7), where a = 0.251 and b = 0.0283, they imply that U_x = 8.87 m s^{-1}. In fact all of the functions presented in Fig. 8 produce very similar values for U_x, all of which are close to 9 m s^{-1}. This value is very close to average wind speed in the North Atlantic (Fig. 3). This is one of the reasons of the small relative difference in net air-sea flux. The spread of flux values for the Southern Ocean seems to support this conclusion, being larger than the North Atlantic one. Southern Ocean has on average stronger winds than North Atlantic (including also the Arctic Seas) which seem to have the smallest spread of flux values for different parameterizations. The other reason is the lack of seasonal variation in the sign of the air-sea flux. In the case of seasonal changes in the air-sea flux direction (caused by seasonal changes in water temperature or primary productivity), with winds stronger than U_x in some seasons and weaker in others (usually strong winds in winter and weak in summer), the air-sea fluxes partly cancel each other while the difference between cubic and quadratic parameterizations add to each other due to simultaneous changes in the sign of both fluxes itself and the U - U_x term. This effect of seasonal variation has been suggested to us based on available observations (A. Watson – personal communication) but we are unaware of any paper investigating it or even describing it explicitly.

In addition to the five parameterizations described above, we calculated the air-sea fluxes using the OceanFlux GHG Evolution combined formula, which parameterises the contributions from direct and bubble-mediated gas transfer into separate components. The resulting air-sea fluxes are higher in absolute terms, than all of the quadratic functions considered in this study, and are closer in value to cubic parameterization. This may mean that the bubble mediated term of Fangohr and Woolf (2007) is overestimating the bubble component, implying the need for a dedicated calibration effort. This question will be the subject of further studies in the OceanFlux Evolution project.

Although, using both Takahashi climatology and SOCAT pCO_2 climatology (Fig. 7) result in similar annual net air-sea fluxes in the North Atlantic, it should be noted that they show different seasonal variations. This may have been caused by slightly different time periods of the datasets (i.e. the SOCAT based climatology contains more recent data). The difference is much larger in the European Arctic due to the underlying sparse data coverage and possible interpolation artifacts (Goddijn-Murphy et al., 2015). This discrepancy makes us treat the net air-sea CO_2 flux results from the Arctic with much less confidence than the values for the whole North Atlantic. It is impossible to declare within this study which dataset is more accurate as only new data can settle this. However, such data have been recently published (Yasunaka et al., 2016). The observed in-water pCO_2 data (Fig. 3 in Yasunaka et al., 2016), especially since 2005, show clearly an annual cycle compatible with the SOCAT seasonal flux variability.

5. Conclusions

In this paper we have studied the effect of the choice of gas transfer velocity parameterization on the net CO_2 air-sea gas fluxes in the North Atlantic and European Arctic using the recently developed FluxEngine software. The results show that the uncertainty caused by the choice of the k formula is smaller in the North Atlantic and in the Arctic than it is globally. The difference in the annual net air-sea CO_2 flux caused by the choice of the parameterization is within 5% in the North Atlantic and 4% in the European Arctic, comparing to 9% globally for the studied functions with quadratic wind dependence. It is up to 46% different for North Atlantic, 36% for Arctic and 65% globally when comparing cubic and quadratic functions. In both cases the uncertainty in the North Atlantic and Arctic regions are smaller than the global case. We explain that the smaller North Atlantic variability is the combination of firstly higher than global average wind speeds in the North Atlantic, close to 9 m s^{-1}, which is the wind speed at which most k parameterization have similar values, and secondly the all-season CO_2 sink conditions in most North Atlantic areas. We repeat the analysis using Takahashi and a SOCAT pCO_2 derived climatology and find that although the seasonal variability in the North Atlantic is different, the annual net air-sea CO_2 fluxes are within

8% in the North Atlantic and 19% in the European Arctic. The seasonal flux calculated from the two *p*CO2 datasets in the Arctic have inverse seasonal variations, indicating possible under sampling (aliasing) of the pCO_2 in this polar region and therefore highlighting the need to collect more polar pCO_2 observations in all months and seasons.

Acknowledgements

The publication has been financed from the funds of the Leading National Research Centre (KNOW) received by the Centre for Polar Studies for the period 2014-2018; OceanFlux Greenhouse Gases Evolution, a project funded by the European Space Agency, ESRIN Contract No. 4000112091/14/I-LG; and GAME "Growing of Marine Arctic Ecosystem", funded by Narodowe Centrum Nauki grant DEC-2012/04/A/NZ8/00661. We would also like to thank Jamie Shutler for important advice on the FluxEngine and for correcting the native-speaker verification of our English.

References

Bakker, D. C. E., Pfeil, B., Smith, K., Hankin, S., Olsen, A., Alin, S. R., Cosca, C., Harasawa, S., Kozyr, A., Nojiri, Y., O'Brien, K. M., Schuster, U., Telszewski, M., Tilbrook, B., Wada, C., Akl, J., Barbero, L., Bates, N. R., Boutin, J., Bozec, Y., Cai, W.-J., Castle, R. D., Chavez, F. P., Chen, L., Chierici, M., Currie, K., de Baar, H. J. W., Evans, W., Feely, R. A., Fransson, A., Gao, Z., Hales, B., Hardman-Mountford, N. J., Hoppema, M., Huang, W.-J., Hunt, C. W., Huss, B., Ichikawa, T., Johannessen, T., Jones, E. M., Jones, S. D., Jutterström, S., Kitidis, V., Körtzinger, A., Landschützer, P., Lauvset, S. K., Lefèvre, N., Manke, A. B., Mathis, J. T., Merlivat, L., Metzl, N., Murata, A., Newberger, T., Omar, A. M., Ono, T., Park, G.-H., Paterson, K., Pierrot, D., Ríos, A. F., Sabine, C. L., Saito, S., Salisbury, J., Sarma, V. V. S. S., Schlitzer, R., Sieger, R., Skjelvan, I., Steinhoff, T., Sullivan, K. F., Sun, H., Sutton, A. J., Suzuki, T., Sweeney, C., Takahashi, T., Tjiputra, J., Tsurushima, N., van Heuven, S. M. A. C., Vandemark, D., Vlahos, P., Wallace, D. W. R., Wanninkhof, R., and Watson, A. J.: An update to the Surface Ocean CO_2 Atlas (SOCAT version 2), Earth Syst. Sci. Data, 6, 69-90, doi:10.5194/essd-6-69-2014, 2014.

Donlon, C. J., Martin, M., Stark, J. D., Roberts-Jones, J., Fiedler, E., and Wimmer, W.: The Operational Sea Surface Temperature and Sea Icea Analysis (OSTIA), Remote Sens. Environ, Special Issue 116, 140-158, doi: 10.1016/j.rse.2010.10.017, 2011.

Fangohr, S. and Woolf, D. K.: Application of new parameterizations of gas transfer velocity and their impact on regional and global CO2 budgets, J. Marine Syst., 66, 195-203, 2007.

Garbe, C. S., Rutgersson, A., Boutin, J., de Leeuw, G., Delille, B., Fairall, C. W., Gruber, N., Hare, J., Ho, D. T., Johnson, M. T., Nightingale, P. D., Pettersson, H., Piskozub, J., Sahlee, E., Tsai, W., Ward, B., Woolf, D. K., and Zappa, C. J.: Transfer Across the Air-Sea Interface, in: Ocean-Atmosphere Interactions of Gases and Particles, edited by: Liss, P. S. and Johnson, M. T., Springer, Earth System Science, Springer, Berlin, Heidelberg, 55–111, 2014.

Goddijn-Murphy L., Woolf D. K., Callaghan A. H.: Parameterizations and Algorithms for Oceanic Whitecap Coverage, J. Phys. Oceanogr., 41, 742-756, 2011.

Goddijn-Murphy, L. M., Woolf, D. K., and Marandino, C.: Space-based retrievals of air-sea gas transfer velocities using altimeters: Calibration for dimethyl sulfide, J. Geophys. Res., 117, C08028, doi: 10.1029/2011JC007535, 2012.

Goddijn-Murphy, L. M., Woolf, D. K., Land, P. E., Shutler J. D., Donlon, C.: The OceanFlux Greenhouse Gases methodology for deriving a sea surface climatology of CO_2 fugacity in support of air-sea gas lux studies, Ocean Sci., 11, 519-541,2015, doi: 10.5194/os-11-519-2015, 2015.

Gonzalez-Davila, M., Santana-Casiano, J. M., and Gonzalez-Davila, E. F.: Interannual variability of the upper ocean carbon cycle in the northeast Atlantic Ocean, Geophys. Res. Lett., 34, L07608, doi: 10.1029/2006GL028145, 2007.

Gregg, W. W., Casey N. W., Rosseaux C. S,: Sensitivity of simulated global ocean carbon flux estimates to forcing by reanalysis products, Ocean Modelling, 80, 24-35, doi: 10.1016/j.ocemod.2014.05.002, 2015.

Gruber, N.: Fickle trends in the ocean, Nature, 458, 155-156, doi: 10.1038/458155a, 2009.

Halloran, P. R., Booth, B. B. B., Jones, C. D., Lambert, F. H., McNeall, D. J., Totterdell, I. J., and Völke, C.: The mechanisms of North Atlantic CO_2 uptake in a large Earth System Model ensemble, Biogeosciences, 12, 4497–4508, doi: 10.5194/bg-12-4497-2015, 2015.

Ho, D., Law C., Smith M., Schlosser P., Harvey M., Hill P.: Measurements of air-sea gas exchange at high wind speeds in the Southern Ocean: Implications for global parametrizations, Geophys. Res. Lett., 33, L16611, doi: 10.1029/2006/GL026817, 2006.

Landschützer, P., Gruber, N., Bakker, D. C. E., Schuster, U., Nakaoka, S., Payne, M. R., Sasse, T. P., and Zeng, J.: A neural network-based estimate of the seasonal to inter-annual variability of the Atlantic Ocean carbon sink, Biogeosciences, 10, 7793-7815, doi: 10.5194/bg-10-7793-2013, 2013.

Landschützer, P., Gruber, N., Bakker, D. C. E., Schuster, U.: Recent variability of the global ocean carbon sink, Global Biogeochem. Cy, 28, 927–949, doi: 10.1002/2014GB004853, 2014.

Le Quéré C., Rodembeck C., Buitenhuise E., Conway T., Langenfelds R., Gomez A., Labuschagne C., Ramonet M., Nakazawa T., Metzle N., Gillett N., heimann M.: Saturation of the Southern Ocean CO_2 sink due to recent climate change. Science 316, 1735-1738, doi:10.1126/science.1136188, 2007.

Le Quéré, C., Moriarty, R., Andrew, R. M., Peters, G. P., Ciais, P., Friedlingstein, P., Jones, S. D., Sitch, S., Tans, P., Arneth, A., Boden, T. A., Bopp, L., Bozec, Y., Canadell, J. G., Chini, L. P., Chevallier, F., Cosca, C. E., Harris, I., Hoppema, M., Houghton, R. A., House, J. I., Jain, A. K., Johannessen, T., Kato, E., Keeling, R. F., Kitidis, V., Klein Goldewijk, K., Koven, C., Landa, C. S., Landschützer, P., Lenton, A., Lima, I. D., Marland, G., Mathis, J. T., Metzl, N., Nojiri, Y., Olsen, A., Ono, T., Peng, S., Peters, W., Pfeil, B., Poulter, B., Raupach, M. R., Regnier, P., Rödenbeck, C., Saito, S., Salisbury, J. E., Schuster, U., Schwinger, J., Séférian, R., Segschneider, J., Steinhoff, T., Stocker, B. D., Sutton, A. J., Takahashi, T., Tilbrook, B., van der Werf, G. R., Viovy, N., Wang, Y.-P., Wanninkhof, R., Wiltshire, A., and Zeng, N.: Global carbon budget 2014, Earth Syst. Sci. Data, 7, 47–85, doi: 10.5194/essd-7-47-2015, 2015.

Lefèvre, N., Watson, A. J., Olsen, A., Rios, A. F., Perez, F. F., Johannessen, T.: A decrease in the sink for atmospheric CO_2 in the North Atlantic, Geophys. Res. Lett., 31, L07306, doi: 10.1029/2003GL018957, 2004.

McGillis, W. R., and Edson, J. B., Hare, J. E., Fairall, C. W.: Direct covariance air-sea CO_2 fluxes, J. Geophys. Res., 106, 729-16, 2001.

Merchant, C. J., Embury, O., Rayner, N. A., Berry, D. I., Corlett, G. K., K., L., Veal, K. L., Kent, E. C., T., L.-J. D., Remedios, J. J., and Saunders, R.: A 20 year independent record of sea surface temperature for climate from Along-Track Scanning Radiometers, J. Geophys. Res., 117, 2012.

Nightingale, P. D., Malin, G., Law, C. S., Watson, A. J., Liss, P. S., Liddicoat, M. I., Boutin, J., and Upstill-Goddard, R. C.: In situ evaluation of air-sea gas exchange parametrizations using novel conservative and volatile tracers, Global Biogeochem. Cy., 14, 373-387, 2000.

Nightingale, P. D., Relationship between wind speed and gas exchange over the ocean: which parameterization should I use?, Raport from Discussion Session at SOLAS Open Science conference in Kiel, http://goo.gl/TrMQkg, 2015.

Orr, J. C., Maier-Reimer, E., Mikolajewicz, U., Monfray, P., Sarmiento, J. L., Toggweiler, J. R., Taylor, N. K., Palmer, J., Gruber, N., Sabine, C. L., Quéré, C. Le., Key, R. M., Boutin, J.: Estimates of anthropogenic carbon uptake from four three-dimensional global ocean models, Global Biogeochem. Cy., 15(1), 43-60, doi: 10.1029/2000GB001273, 2001.

Pérez, F. F., Herlé Mercier, Marcos Vázquez-Rodríguez, Pascale Lherminier, Anton Velo, Paula C. Pardo, Gabriel Rosón and Aida F. Ríos: Atlantic Ocean CO_2 uptake reduced by weakening of the meridional overturning circulation, Nat. Geosci., 6, 146-152, doi: 10.1038/NGEO1680, 2013.

Pfeil, B., Olsen, A., Bakker, D. C. E., Hankin, S., Koyuk, H., Kozyr, A., Malczyk, J., Manke, A., Metzl, N., Sabine, C. L., Akl, J., Alin, S. R., Bates, N., Bellerby, R. G. J., Borges, A., Boutin, J., Brown, P. J., Cai, W.-J., Chavez, F. P., Chen, A., Cosca, C., Fassbender, A. J., Feely, R. A., González-Dávila, M., Goyet, C., Hales, B., Hardman-Mountford, N., Heinze, C., Hood, M., Hoppema, M., Hunt, C. W., Hydes, D., Ishii, M., Johannessen, T., Jones, S. D., Key, R. M., Körtzinger, A., Landschützer, P., Lauvset, S. K., Lefèvre, N., Lenton, A., Lourantou, A., Merlivat, L., Midorikawa, T., Mintrop, L., Miyazaki, C., Murata, A., Nakadate, A., Nakano, Y., Nakaoka, S., Nojiri, Y., Omar, A. M., Padin, X. A., Park, G.-H., Paterson, K., Perez, F. F., Pierrot, D., Poisson, A., Ríos, A. F., Santana-Casiano, J. M., Salisbury, J., Sarma, V. V. S. S., Schlitzer, R., Schneider, B., Schuster, U., Sieger, R., Skjelvan, I., Steinhoff, T., Suzuki, T., Takahashi, T., Tedesco, K., Telszewski, M., Thomas, H., Tilbrook, B., Tjiputra, J., Vandemark, D., Veness, T., Wanninkhof, R., Watson, A. J., Weiss, R., Wong, C. S., and Yoshikawa-Inoue, H.: A uniform, quality controlled Surface Ocean CO_2 Atlas (SOCAT), Earth Syst. Sci. Data, 5, 125-143, doi: 10.5194/essd-5-125-2013, 2013.

Sabine, C. L., Hankin, S., Koyuk, H., Bakker, D. C. E., Pfeil, B., Olsen, A., Metzl, N., Kozyr, A., Fassbender, A., Manke, A., Malczyk, J., Akl, J., Alin, S. R., Bellerby, R. G. J., Borges, A., Boutin, J., Brown, P. J., Cai, W.-J., Chavez, F. P., Chen, A., Cosca, C., Feely, R. A., González-Dávila, M., Goyet, C., Hardman-Mountford, N., Heinze, C., Hoppema, M., Hunt, C. W., Hydes, D., Ishii, M., Johannessen, T., Key, R. M., Körtzinger, A., Landschützer, P., Lauvset, S. K., Lefèvre, N., Lenton, A., Lourantou, A., Merlivat, L., Midorikawa, T., Mintrop, L., Miyazaki, C., Murata, A., Nakadate, A., Nakano, Y., Nakaoka, S., Nojiri, Y., Omar, A. M., Padin, X. A., Park, G.-H., Paterson, K., Perez, F. F., Pierrot, D., Poisson, A., Ríos, A. F., Salisbury, J., Santana-

Casiano, J. M., Sarma, V. V. S. S., Schlitzer, R., Schneider, B., Schuster, U., Sieger, R., Skjelvan, I., Steinhoff, T., Suzuki, T., Takahashi, T., Tedesco, K., Telszewski, M., Thomas, H., Tilbrook, B., Vandemark, D., Veness, T., Watson, A. J., Weiss, R., Wong, C. S., and Yoshikawa-Inoue, H.: Surface Ocean CO_2 Atlas (SOCAT) gridded data products, Earth Syst. Sci. Data, 5, 145-153, doi: 10.5194/essd-5-145-2013, 2013.

Schuster, U., and Watson, A. J.: A variable and decreasing sink for atmospheric CO_2 in the North Atlantic, J. Geophys. Res., 112, C11006, doi: 10.1029/2006JC003941, 2007.

Schuster, U., McKinley, G. A., Bates, N., Chevallier, F., Doney, S. C., Fay, A. R., Gonzalez-Davila, M., Gruber, N., Jones, S., Krijnen, J., Landschutzer, P., Lefèvre, N., Manizza, M., Mathis, J., Metzl, N., Olsen, A., Rios, A. F., Rodenbeck, C., Santana-Casiano, J. M., Takahashi, T., Wanninkhof, R., and Watson, A. J.: An assessment of the Atlantic and Arctic sea–air CO_2 fluxes, 1990–2009, Biogeosciences, 10, 607–627, doi: 10.5194/bg-10-607-2013, 2013.

Shutler, J. D., Piolle, J-F., Land, P. E., Woolf, D. K., Goddijn-Murphy, L., Paul, F., Girard-Ardhuin, F., Chapron, B., and Donlon, C. J.: FluxEngine: a flexible processing system for calculating air-sea carbon dioxide gas fluxes and climatologies, J. Atmos. Ocean. Tech., http://dx.doi.org/10.1175/JTECH-D-14-00204.1, 2016.

Sweeney, C., Gloor, E., Jacobson, A. R., Key, R. M., McKinley, G., Sarmiento, J. L. and Wanninkhof, R.: Constraining global air-sea gas exchange for CO_2 with recent bomb 14C measurements, Global Biogeochem. Cycles, 21, GB2015, http://dx.doi.org/10.1029/2006GB002784, 2007.

Takahashi, T., Sutherland, S. G., Sweeney, C., Poisson, A. P., Metzl, N., Tilbrook, B., Bates, N. R., Wanninkhof, R., Feely, R. A., Sabine, C. L., Olafsson, J., and Nojjiri, Y.: Global sea-air CO_2 flux based on climatological surface ocean pCO_2, and seasonal biological and temperature effects, Deep Sea Res., Pt. II, 49, 1601-1622, 2002.

Takahashi, T., Sutherland, S. C., Wanninkhof, R., Sweeney, C., Feely, R. A., Chipman, D. W., Hales, B., Friederich, G., Chavez, F., Sabine, C., Watson, A., Bakker, D. C. E., Schuster, U., Metzl, N., Inoue, H. Y., Ishii, M., Midorikawa, T., Nojiri, Y., Koertzinger, A., Steinhoff, T., Hoppema, M., Olafsson, J., Arnarson, T. S., Tilbrook, B., Johannessen, T., Olsen, A., Bellerby, R., Wong, C. S., Delille, B., Bates, N. R., and de Baar, H. J. W.: Climatological mean and decadal change in surface ocean pCO_2 and net sea-air CO_2 flux over the global oceans, Deep-Sea Res. Pt. II, 56, 554–577, doi: 10.1016/j.dsr2.2008.12.009, 2009.

Talley, L. D.: Closure of the Global Overturning Circulation Through the Indian, Pacific, and Southern Oceans: Schematics and Transports, Oceanography 26(1), 80–97, doi:10.5670/oceanog.2013.07, 2013.

Thomas, H., Friederike Prowe, A. E., Lima, I. D., Doney, S. C., Wanninkhof, R., Greatbatch, R. J., Schuster, U., and Corbiere, A.: Changes in the North Atlantic Oscillation influence CO_2 uptake in the North Atlantic over the past 2 decades, Global Biogeochem. Cy., 22, GB4027, doi:10.1029/2007GB003167, 2008.

Wanninkhof, R.: Relationship between wind speed and gas exchange over the ocean revisited, Limnol. Oceanogr.- Meth., 12, 351–362, 2014.

Wanninkhof, R., and McGillis, W. R.: A cubic relationship between air-sea CO_2 exchange and wind speed, Geophys. Res. Lett., 26, 1889-1892, 1999.

Wanninkhof, R., Park, G.-H., Takahashi, T., Sweeney, C., Feely, R., Nojiri, Y., Gruber, N., Doney, S. C., McKinley, G. A., Lenton, A., Quéré C. Le, Heinze, C., Schwinger, J., Graven, H., Khatiwala, S.: Global ocean carbon uptake: magnitude, variability and trends, Biogeosciences, 10, 1987-2013, doi: 10.5194/bg-10-1987-2013, 2013.

Watson, A. J., Schuster, U., Bakker, D. C. E., Bates, N. R., Corbière, A., González-Dávila, M., Friedrich, T., Hauck, J., Heinze, C., Johannessen, T., Körtzinger, A., Metzl, N., Olafsson, J., Olsen, A., Oschlies, A., Padin, X.A., Pfeil, B., Santana-Casiano, J.M., Steinhoff, T., Telszewski, M., Rios, A.F., Wallace, D.W., Wanninkhof, R.: Tracking the variable North Atlantic sink for atmospheric CO_2, Science, 326(5958), 1391-1393, doi: 10.1126/science.1177394, 2009.

Watson, A. J., Metzl, N., Schuster, U.,: Monitoring and interpreting the ocean uptake of atmospheric CO_2, Philos. T. R. Soc. A, 369, 1997–2008, doi: 10.1098/rsta.2011.0060, 2011.

Woolf, D. K.: Parameterization of gas transfer velocities and sea-state dependent wave breaking. Tellus B, 57, 87–94, 2005.

Woolf, D. K., Shutler, J. D., Goddijn-Murphy, L., Donlon, C. J., Nightingale, P. D., Land, P. E., Torres, R., Chapron, B., Piolle, J-F., Herledan, S., Hanafin, J., Girard-Ardhuin, F., Ardhuin, F., Prytherch, J., Moat, B., and Yelland, M.,: Key uncertainties in the contemporary air-sea flux of carbon dioxide: an OceanFlux study, submitted 2015a.

Woolf, D. K., Goddijn-Murphy, L. M., Shutler, J. D., Land, P. E., Donlon, C. J., Prytherch, J., Yelland, M. J., Nightingale, P. D., Torres, R., Chapron, B., Piolle, J-F., Herledan, S., Hanafin, J., Girard-Ardhuin, F., Ardhuin F., and Moat, B.,: Sources and types of uncertainty in the contemporary air-sea flux of carbon dioxide: an OceanFlux study, submitted 2015b.

Yasunaka, S, A. Murata, E. Watanabe, M. Chierici, A. Fransson, S. van Heuven, M. Hoppema, M. Ishii, T. Johannessen, N. Kosugi, S. K. Lauvset, J. T. Mathis, S. Nishino, A. M. Omar, A. Olsen, D. Sasano, T. Takahashi, R. Wanninkhof.,: Mapping of the air–sea CO2 flux in the Arctic Ocean and its adjacent seas: Basin-wide distribution and seasonal to interannual variability, doi:10.1016/j.polar.2016.03.006, 2016

Figure 1. Seasonal and annual mean air-sea fluxes of CO_2 (mg C m^{-2} day^{-1}) in the North Atlantic, using Nightingale et al. (2000) k parameterization and Takahashi (2009) climatology in a) annual, b) DJF (Winter), c) MAM (Spring), d) JJA (Summer), e) SON (Autumn). The gaps (white areas) are due to missing data, land and ice masks.

Figure 2. Seasonal and annual pCO_2 values (μatm) in surface waters of the North Atlantic, estimated using the Takahashi (2009) climatology in a) annual, b) DJF (Winter), c) MAM (Spring), d) JJA (Summer), e) SON (Autumn). The gaps (white areas) are due to missing data, land and ice masks.

Figure 3. Wind speed distribution U_{10} (ms^{-1}) in the North Atlantic used to determine the relationship between gas transfer velocity and air-sea CO_2 fluxes in a) annual, b) DJF (Winter), c) MAM (Spring), d) JJA (Summer), e) SON (Autumn). The gaps (white areas) are due to missing data, land and ice masks.

Figure 4. Differences maps for the air-sea CO_2 fluxes (mg C m^{-2} day^{-1}) in the North Atlantic, between a wind cubed and squared parameterizations (Wanninkhof and McGillis 1999 and Wanninkhof 2014) in a) annual, b) DJF (Winter), c) MAM (Spring), d) JJA (Summer) e) SON (Autumn). The gaps (white areas) are due to missing data, land and ice masks.

Figure 5. Monthly values air-sea fluxes of CO_2 (Pg $month^{-1}$) for the five parameterizations (eq. 4-8) in a) North Atlantic, b) European Arctic.

Figure 6. Annual air-sea fluxes of CO_2 for the five (eq. 4-8) parameterizations as well as for backscatter (default) and wind driven OceanFluxGHG parameterization normalized to flux values of Nightingale et al. (2000) *k* parameterization (see text) in a) global, b) North Atlantic c) European Arctic, d) Southern Ocean. Average values for all parameterization and standard deviations are marked as vertical gray lines. .

Figure 7. Comparison of monthly values fluxes of air-sea CO_2 fluxes calculated with different pCO_2 datasets (Takahashi et al., 2009, SOCAT v. 1.5 and 2.0) using the same *k* parameterization (Nightingale et al., 2000) in a) North Atlantic, b) European Arctic.

Figure 8. Different k660 parameterizations as a function of wind speed.

Table 1. Annual air-sea CO2 fluxes (in Pg) using different k parameterizations. The values in parentheses are fluxed normalized to Nightingale et al., 2000 (as in Fig. 6)

	Global	Arctic	North Atlantic	Southern Ocean
Nightingale et al., 2000	-1.30 (1.00)	-0.102 (1.00)	-0.382 (1.00)	-0.72 (1.00)
Ho et al., 2006	-1.42 (1.09)	-0.106 (1.04)	-0.402 (1.05)	-0.76 (1.06)
Wanninkhof and McGillis, 1999	-1.73 (1.33)	-1.130 (1.28)	-0.490 (1.29)	-0.93 (1.30)
Wanninkhof, 2014	-1.40 (1.08)	-0.105 (1.03)	-0.398 (1.04)	-0.76 (1.05)
McGillis et al., 2001	-2.15 (1.65)	-0.147 (1.44)	-0.557 (1.46)	-1.08 (1.49)
OceanFlux GHG wind driven	-1.98 (1.52)	-0.138 (1.36)	-0.560 (1.47)	-1.14 (1.58)
OceanFluxGHG backscatter	-1.88 (1.44)	-0.130 (1.27)	-0.526 (1.38)	-1.09 (1.51)

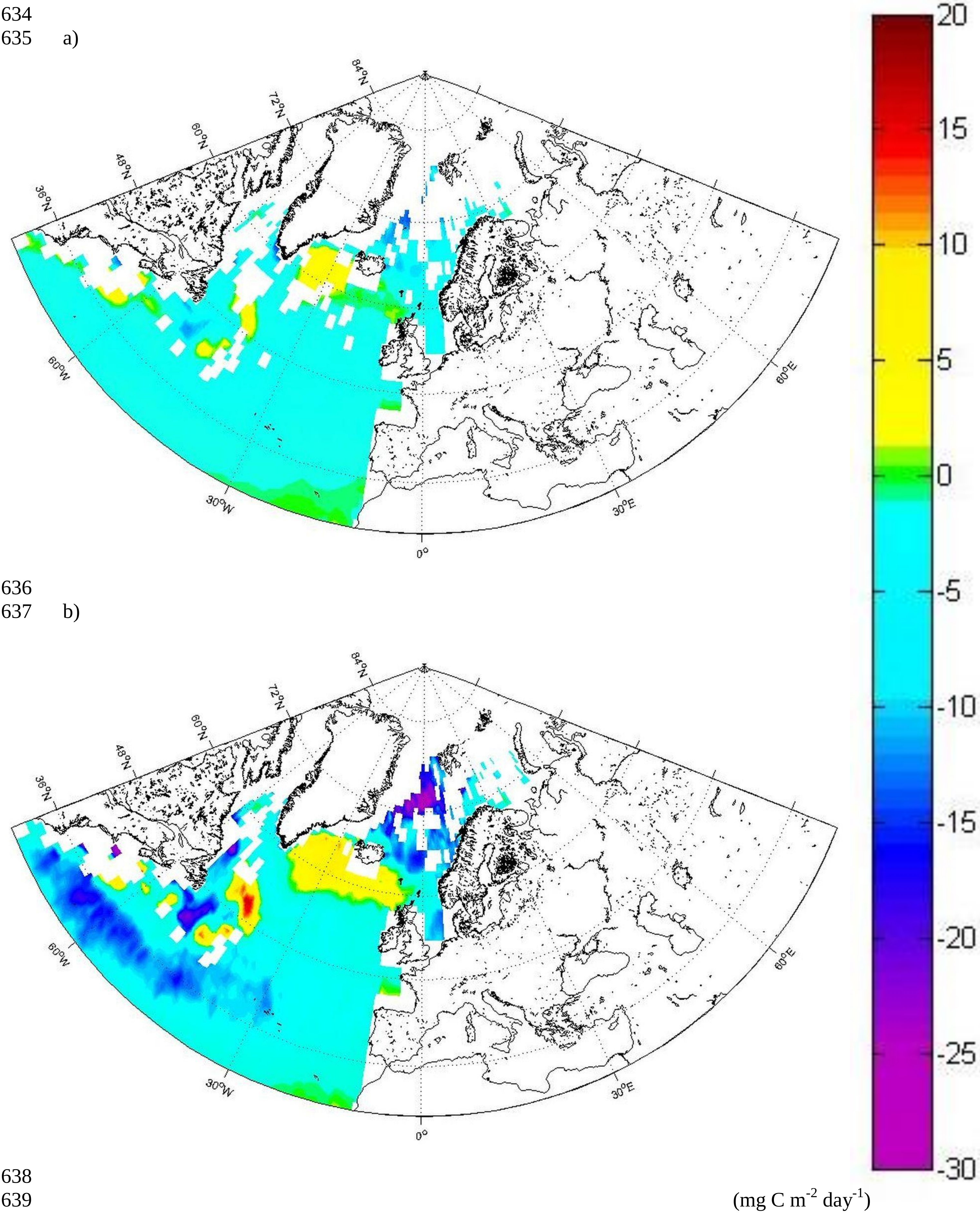
a)
84°N
72°N
60°N
48°N
36°N
60°W
30°W
0°
30°E
60°E
b)
84°N
72°N
60°N
48°N
36°N
60°W
30°W
0°
30°E
60°E
20
15
10
5
0
-5
-10
-15
-20
-25
-30
(mg C m-2 day-1)

c)

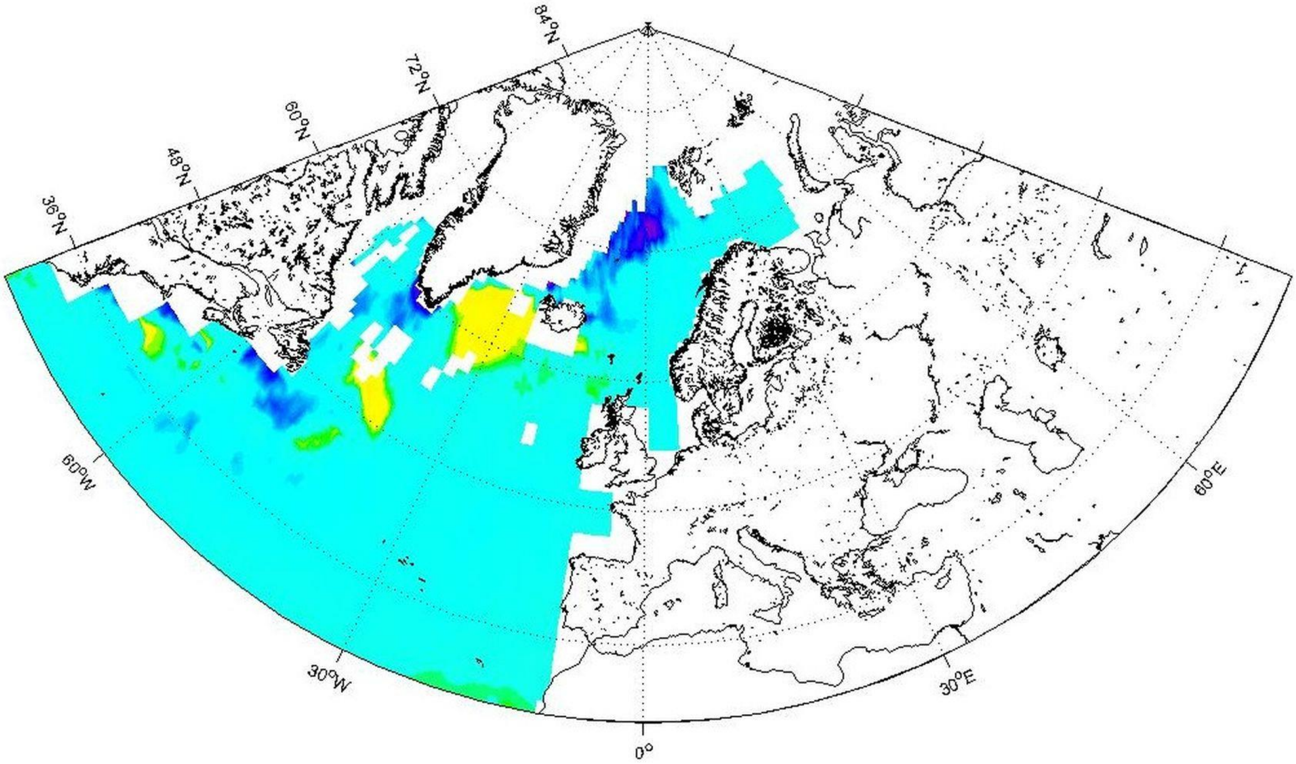

d)

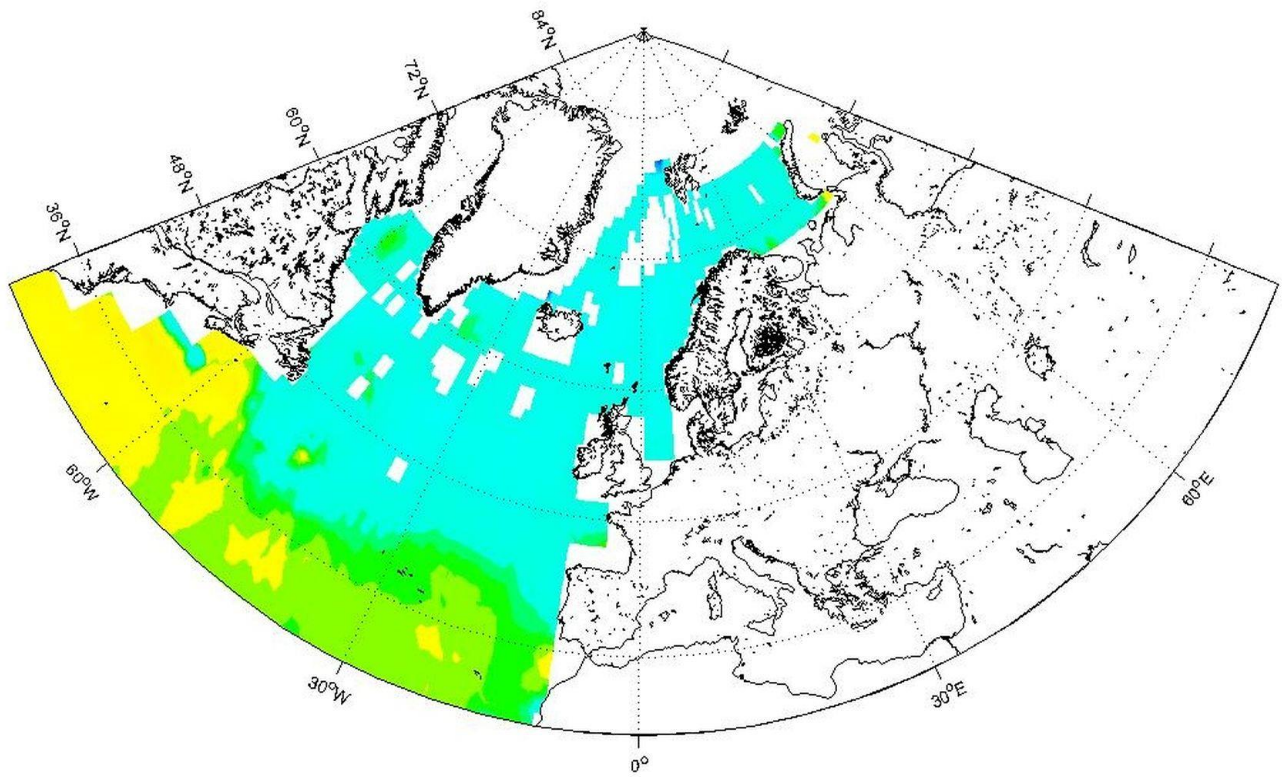

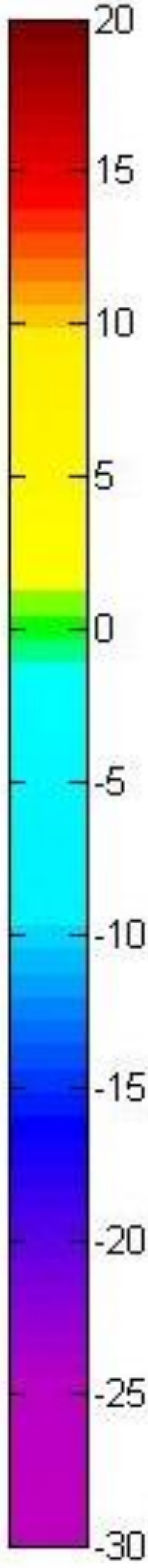

(mg C m^{-2} day^{-1})

e)

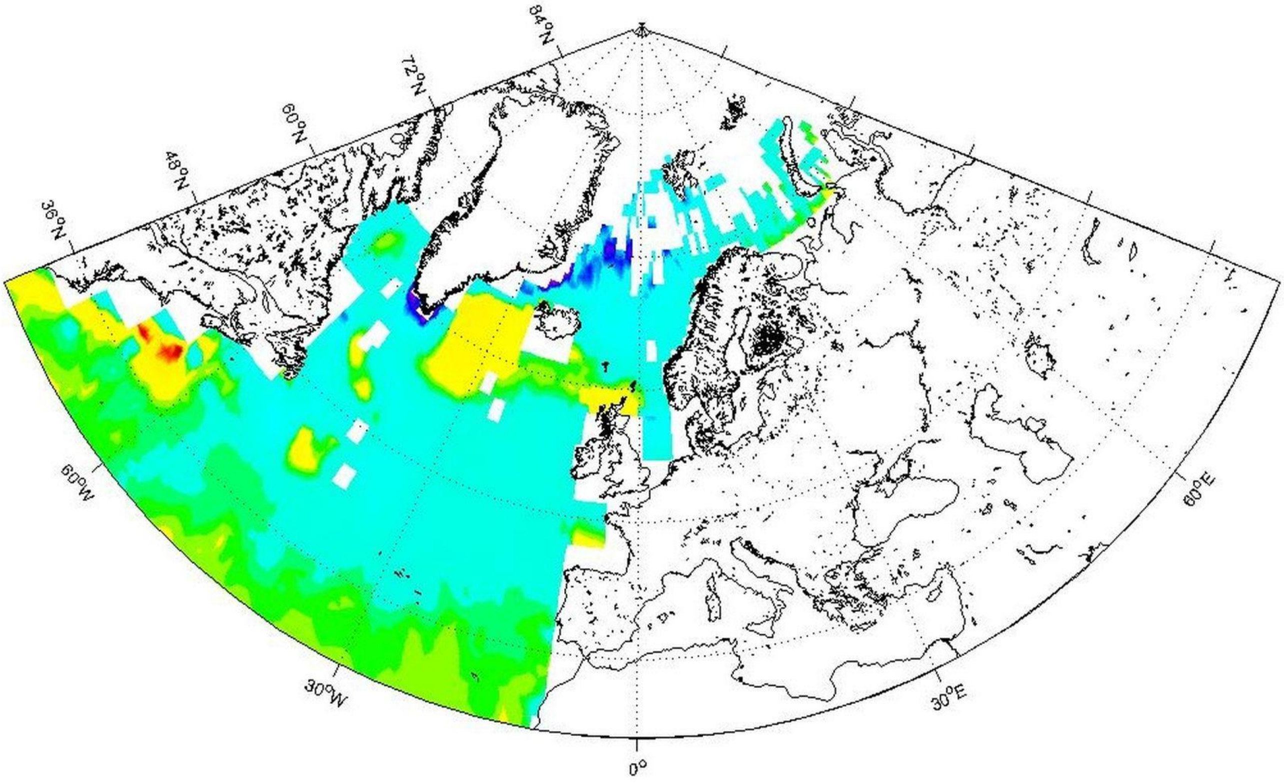

Figure 1. Seasonal and annual mean air-sea fluxes of CO_2 (mg C m^{-2} day^{-1}) in the North Atlantic, combine using Nightingale et al. (2000) *k* parameterization and the Takahashi (2009) climatology in a) annual, b) DJF (Winter), c) MAM (Spring), d) JJA (Summer), e) SON (Autumn). The gaps (white areas) are due to missing data, land and ice masks.

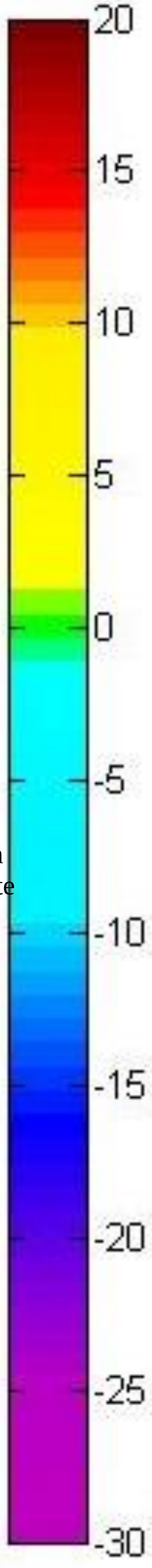

(mg C m^{-2} day^{-1})

a)

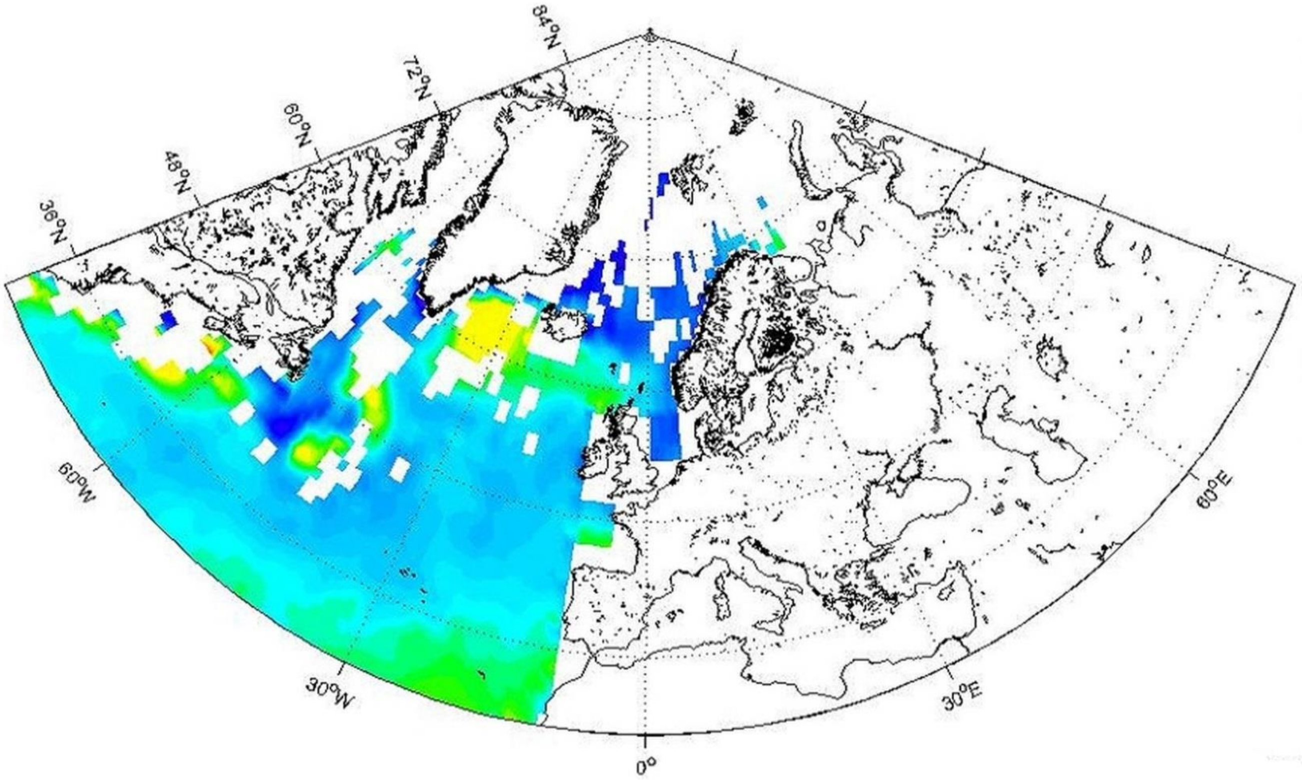
84°N
72°N
60°N
48°N
36°N
60°W
30°W
0°
30°E
60°E

b)

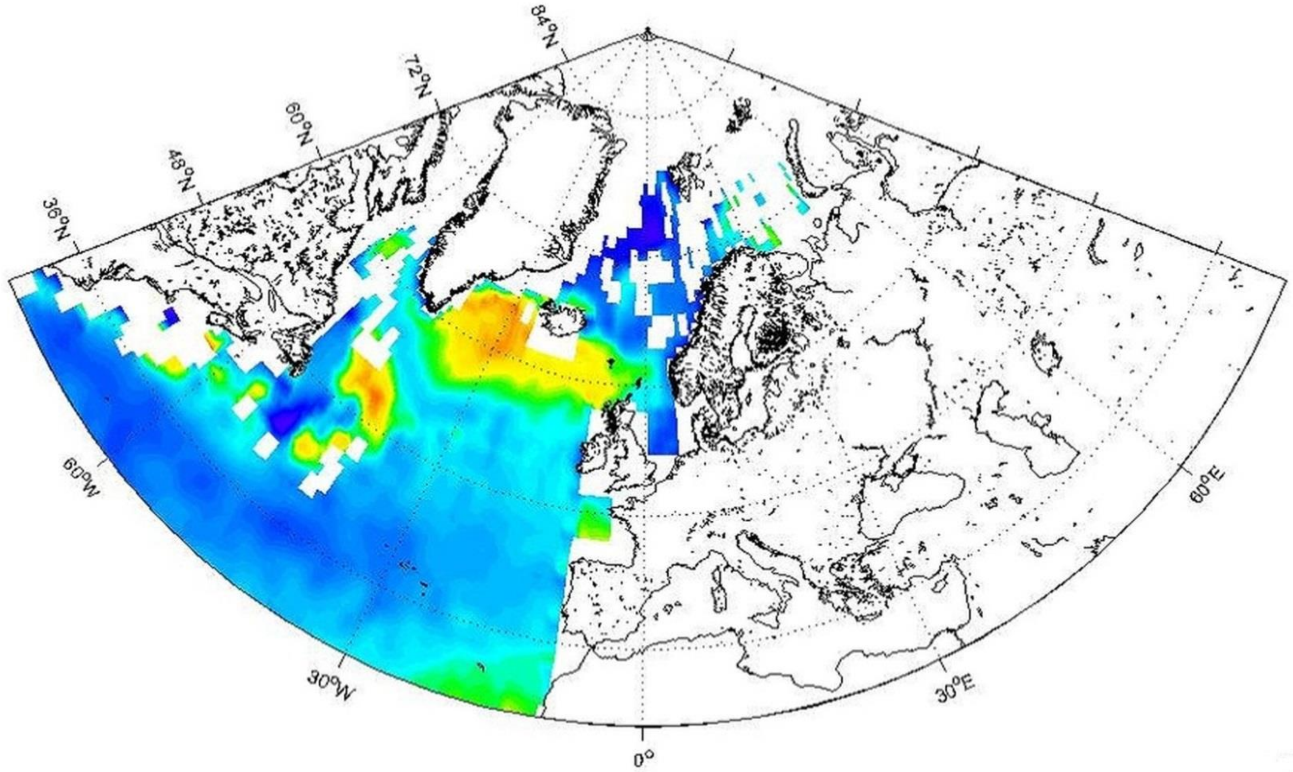
84°N
72°N
60°N
48°N
36°N
60°W
30°W
0°
30°E
60°E

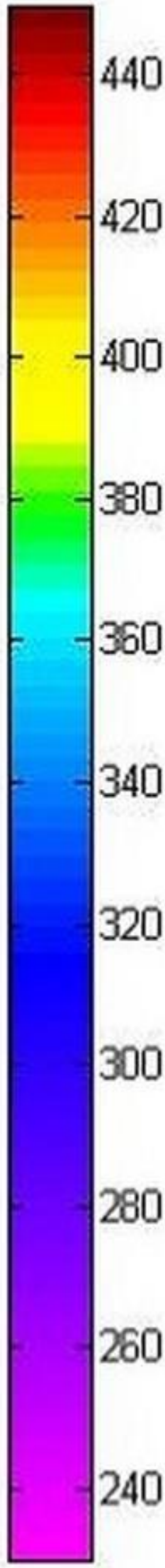
440
420
400
380
360
340
320
300
280
260
240

(µatm)

c)

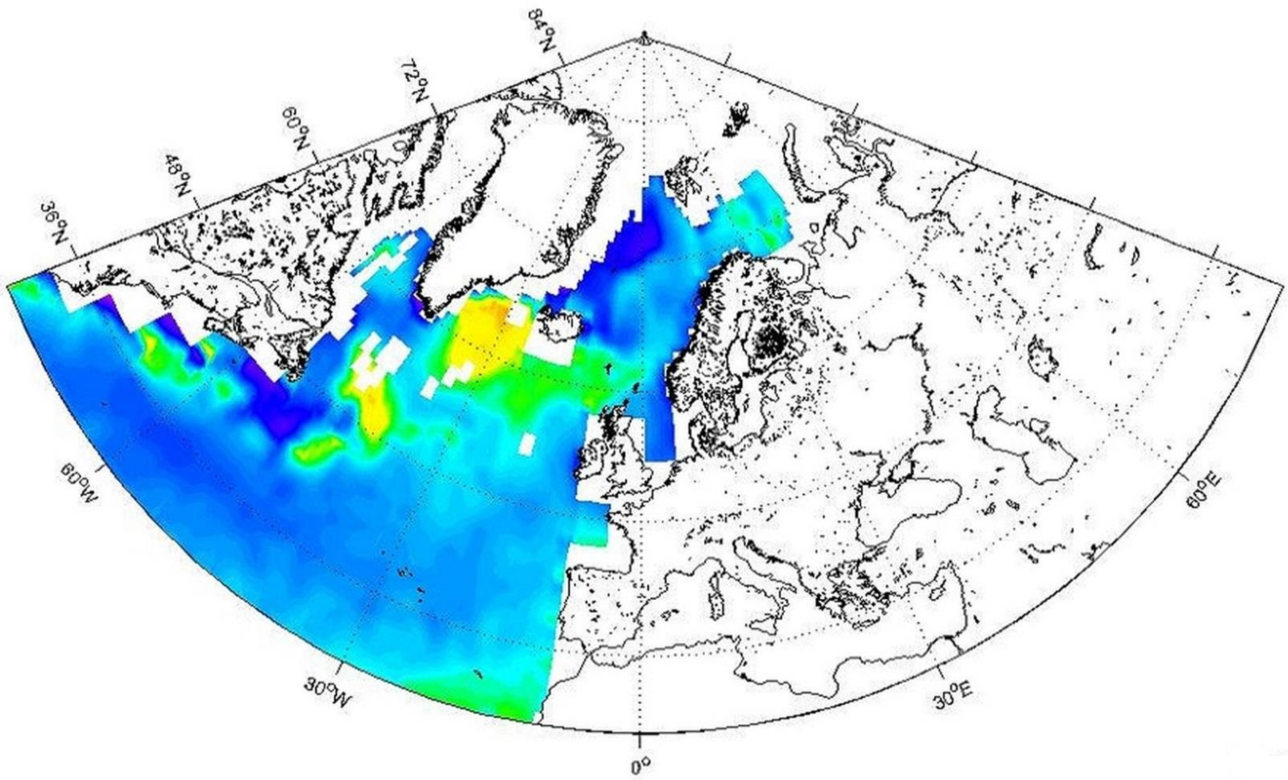
84°N
72°N
60°N
48°N
36°N
60°W
30°W
0°
30°E
60°E

d)

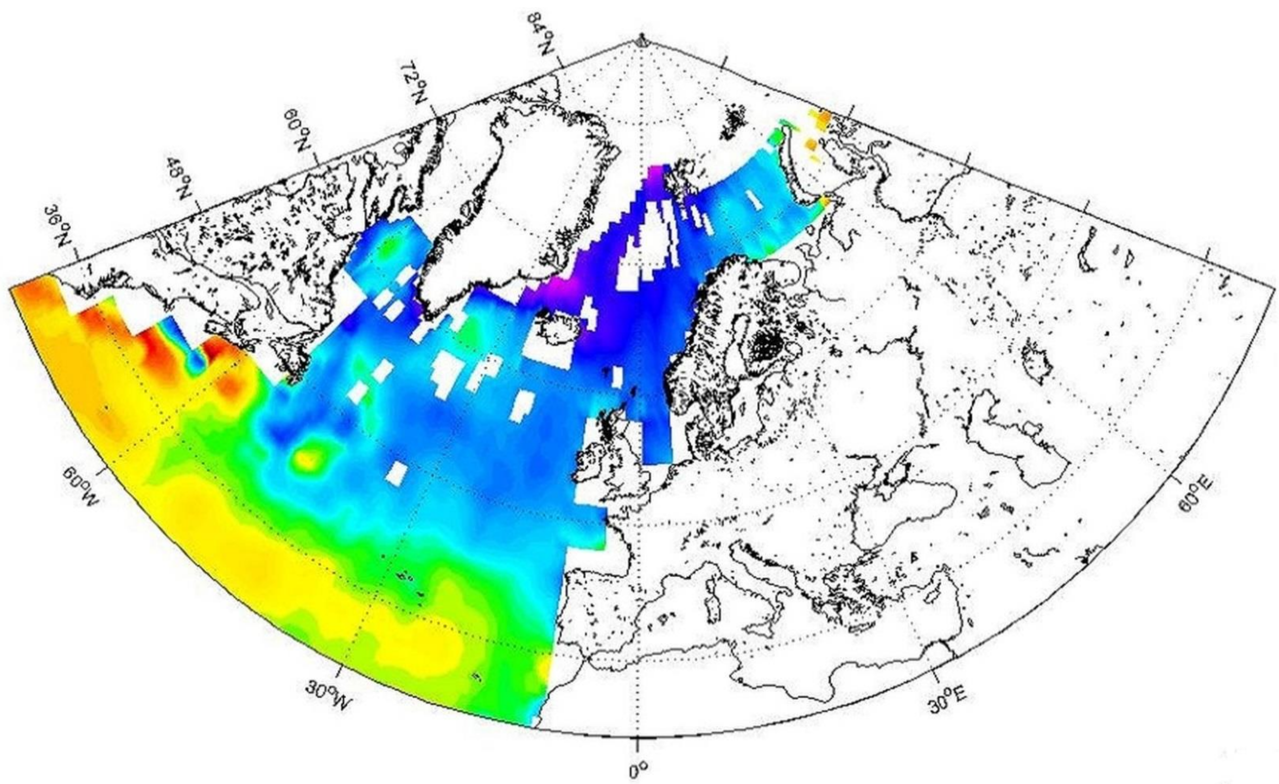
84°N
72°N
60°N
48°N
36°N
60°W
30°W
0°
30°E
60°E

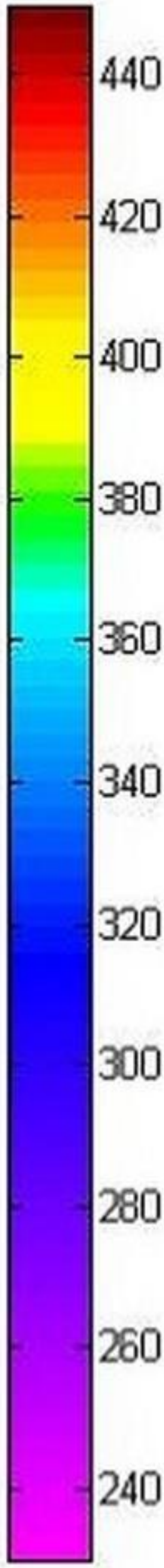
440
420
400
380
360
340
320
300
280
260
240

(µatm)

e)

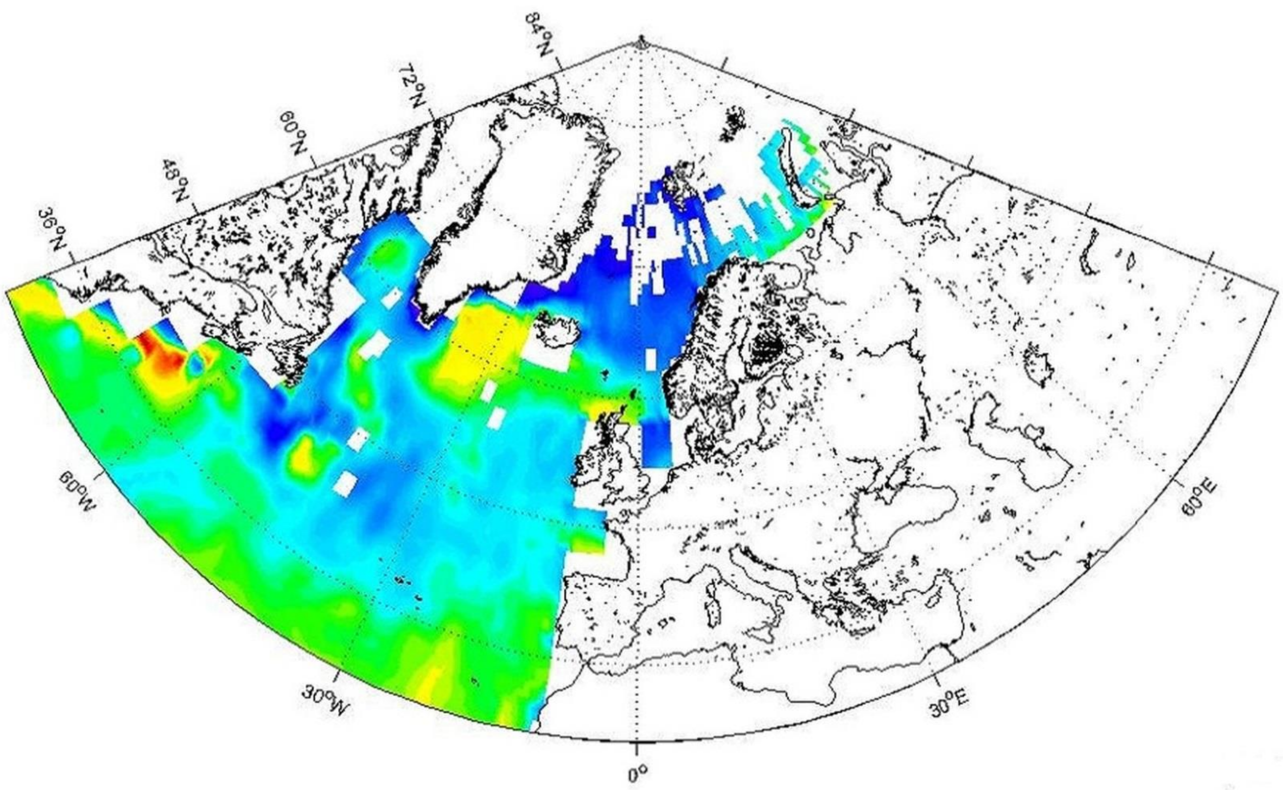

Figure 2. Seasonal and annual pCO_2 values (μatm) in surface waters of the North Atlantic, estimated using Takahashi (2009) climatology in a) annual, b) DJF (Winter), c) MAM (Spring), d) JJA (Summer), e) SON (Autumn). The gaps (white areas) are due to missing data, land and ice masks.

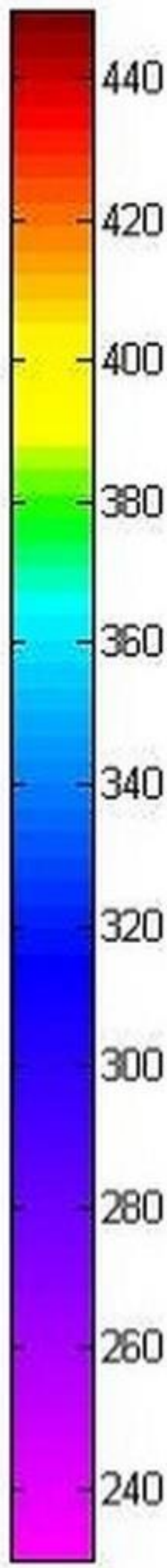

(μatm)

a)

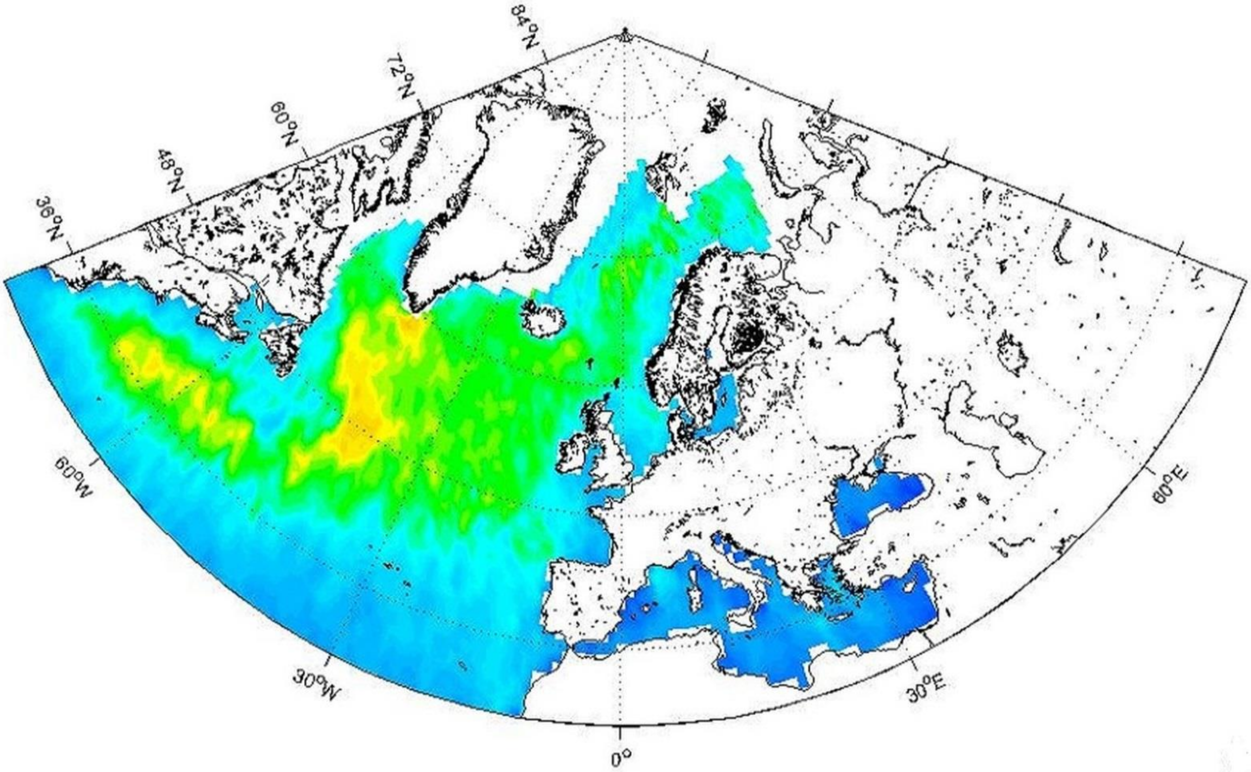
84°N
72°N
60°N
48°N
36°N
60°W
30°W
0°
30°E
60°E

b)

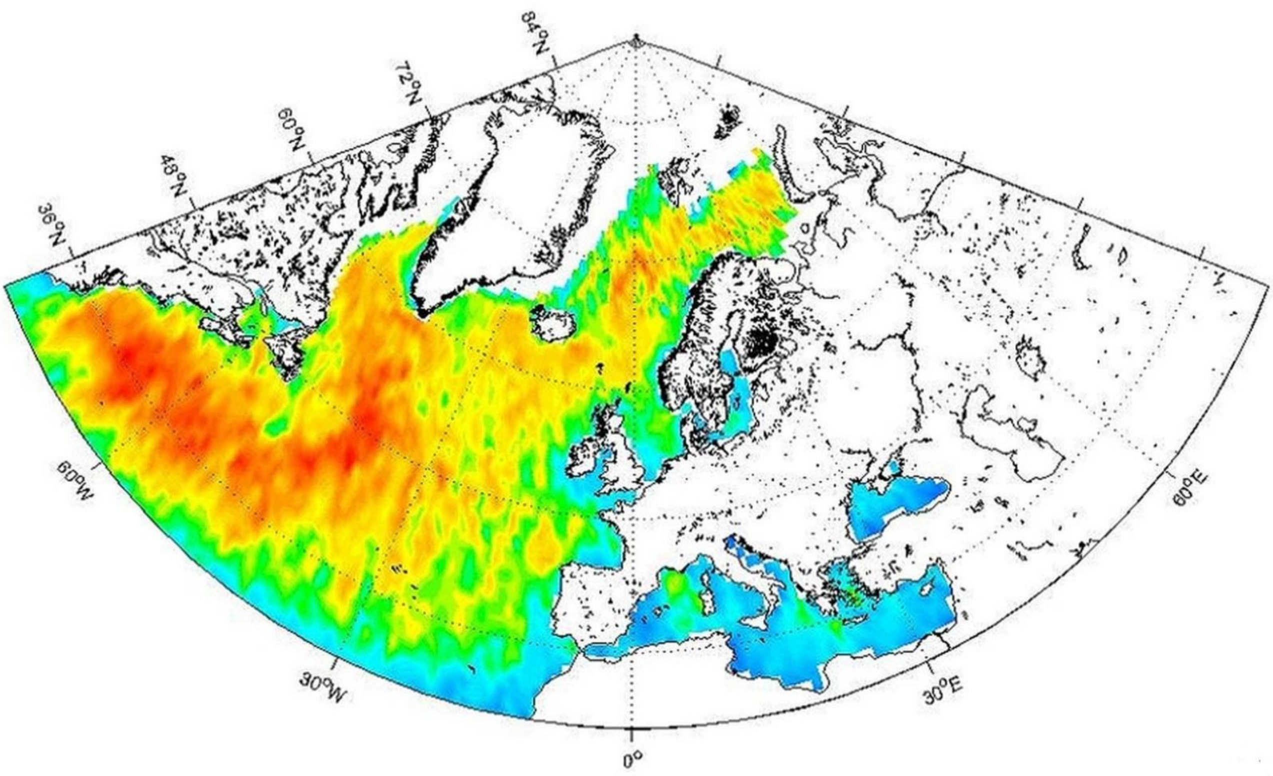
84°N
72°N
60°N
48°N
36°N
60°W
30°W
0°
30°E
60°E

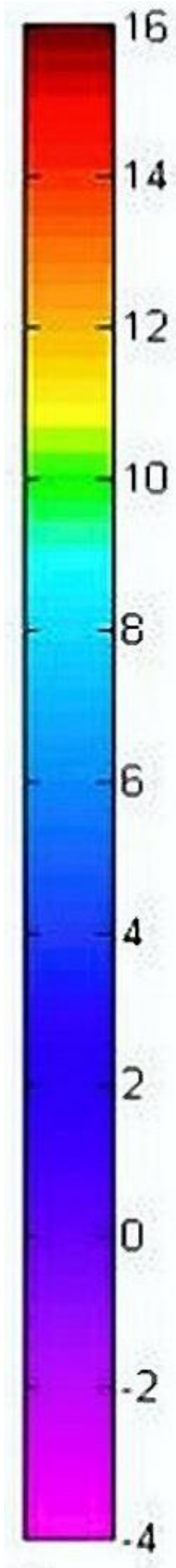
16
14
12
10
8
6
4
2
0
-2
-4

(ms^{-1})

c)

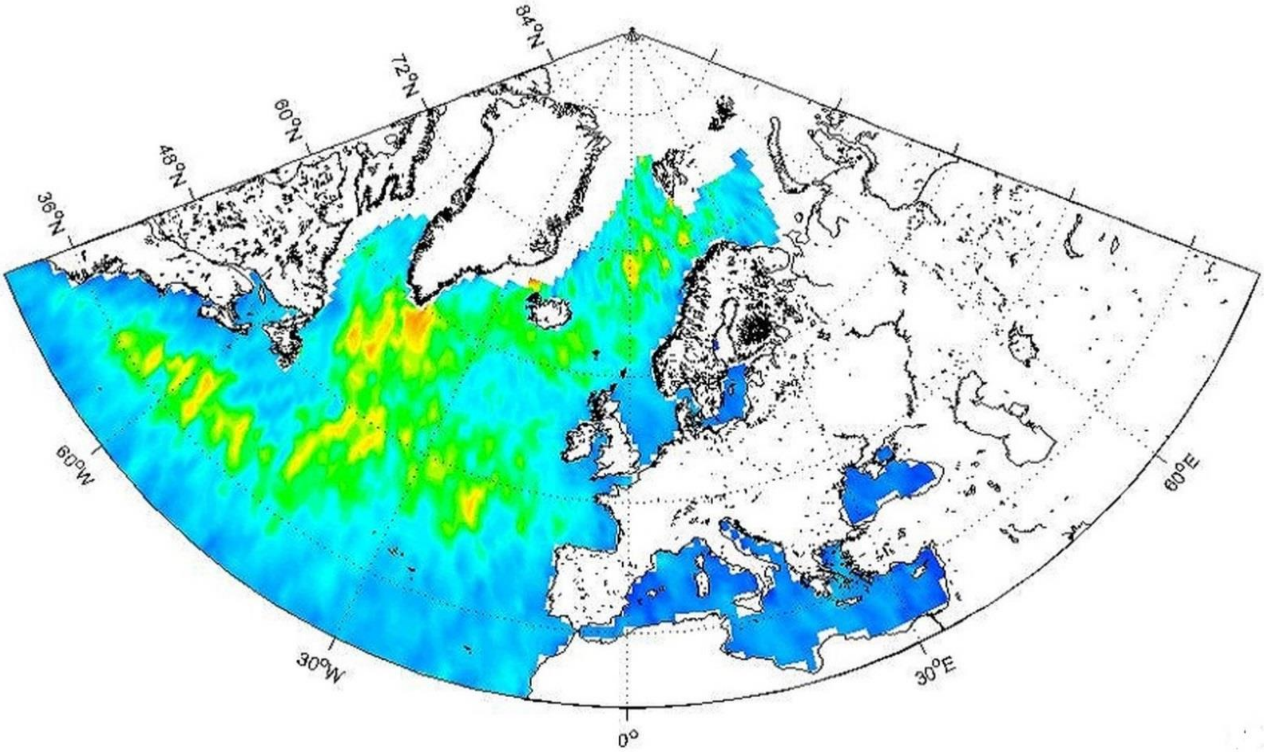
84°N
72°N
60°N
48°N
36°N
60°W
30°W
0°
30°E
60°E

d)

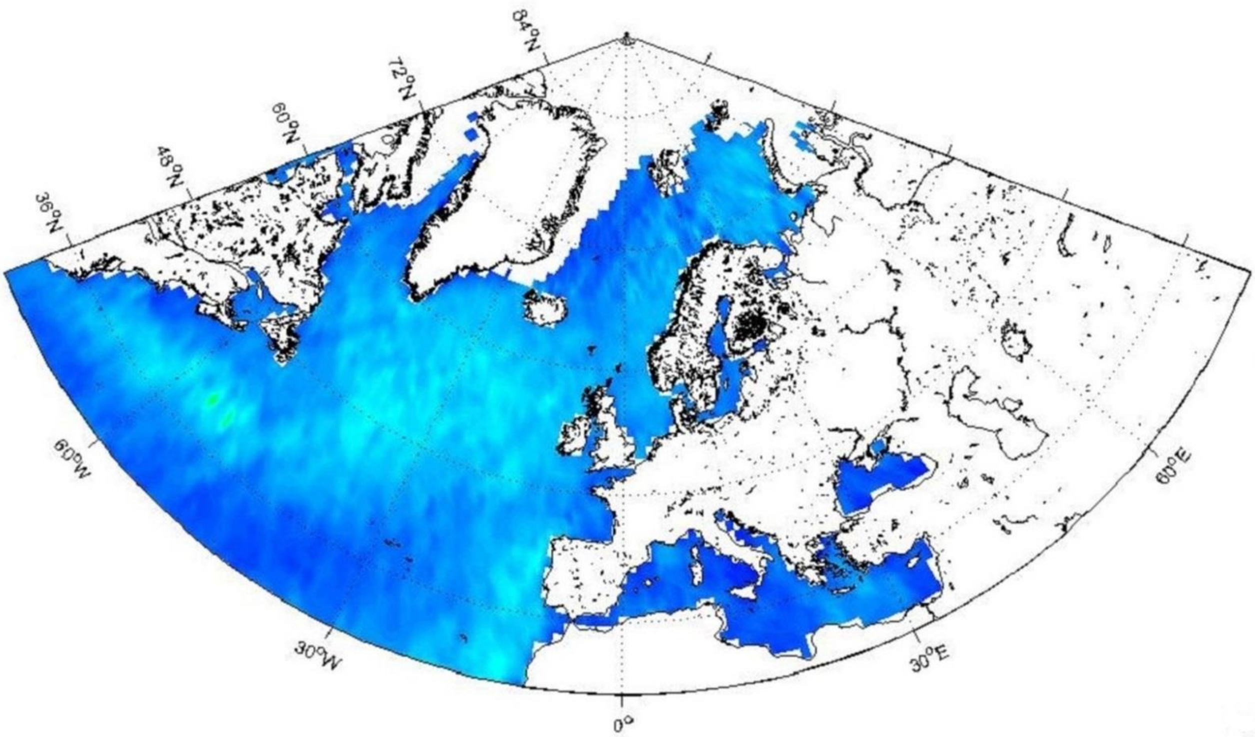
84°N
72°N
60°N
48°N
36°N
60°W
30°W
0°
30°E
60°E

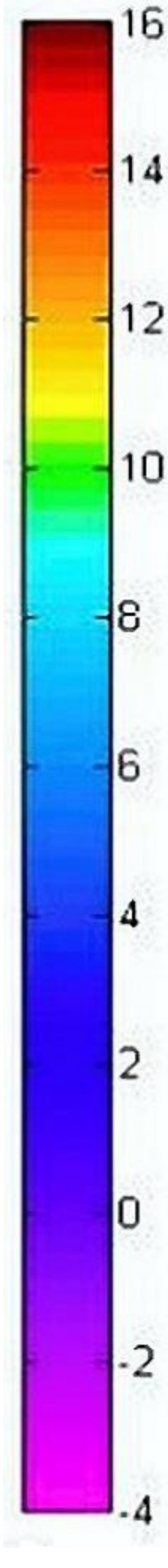
16
14
12
10
8
6
4
2
0
-2
-4

(ms^{-1})

e)

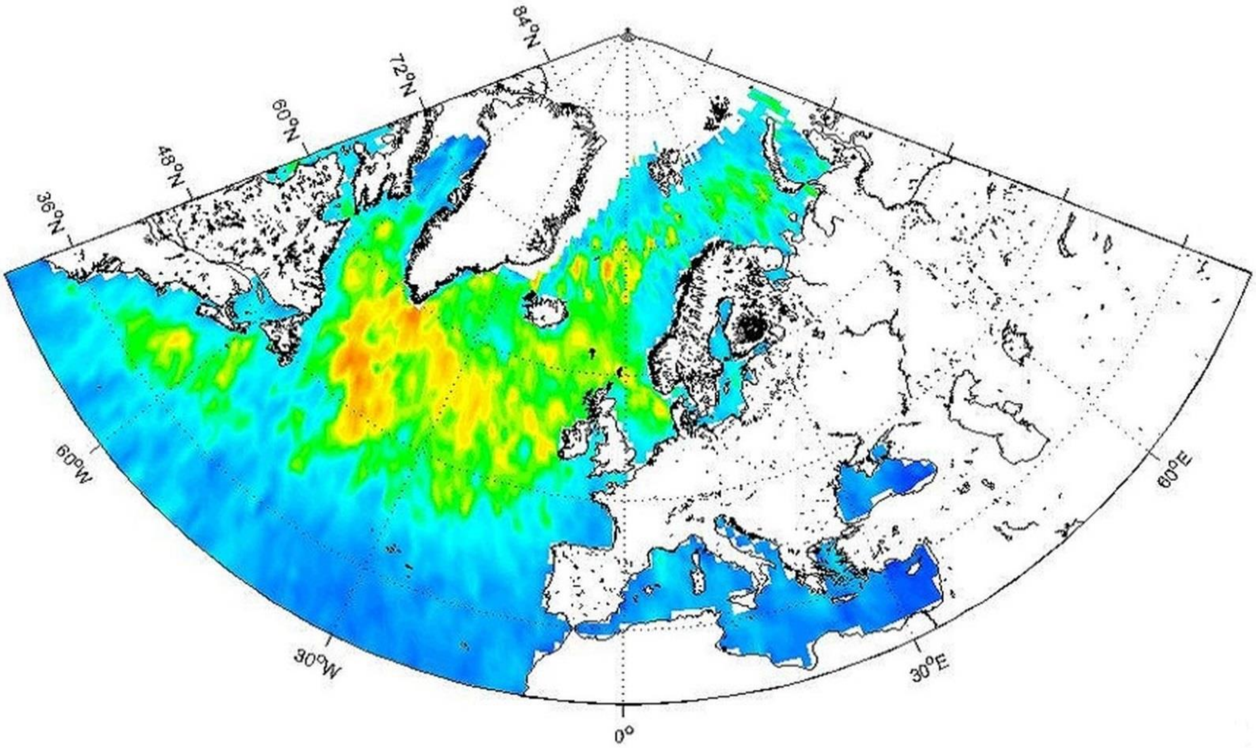

Figure 3. Wind speed distribution U_{10} (ms^{-1}) in the North Atlantic used to determine the relationship between gas transfer velocity and air-sea CO_2 fluxes in a) annual, b) DJF (Winter), c) MAM (Spring), d) JJA (Summer), e) SON (Autumn). The gaps (white areas) are due to missing data, land and ice masks.

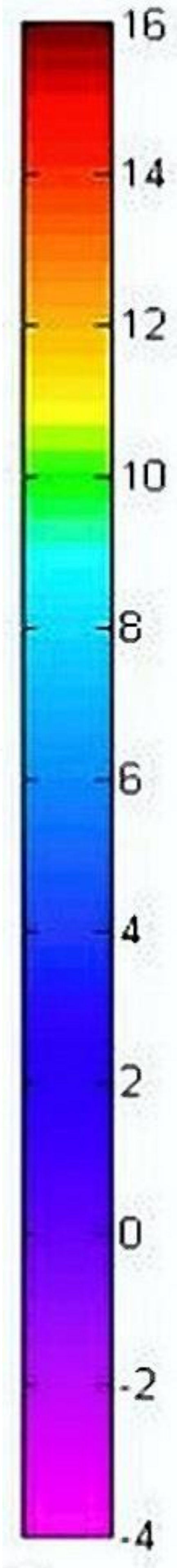

(ms^{-1})

a)

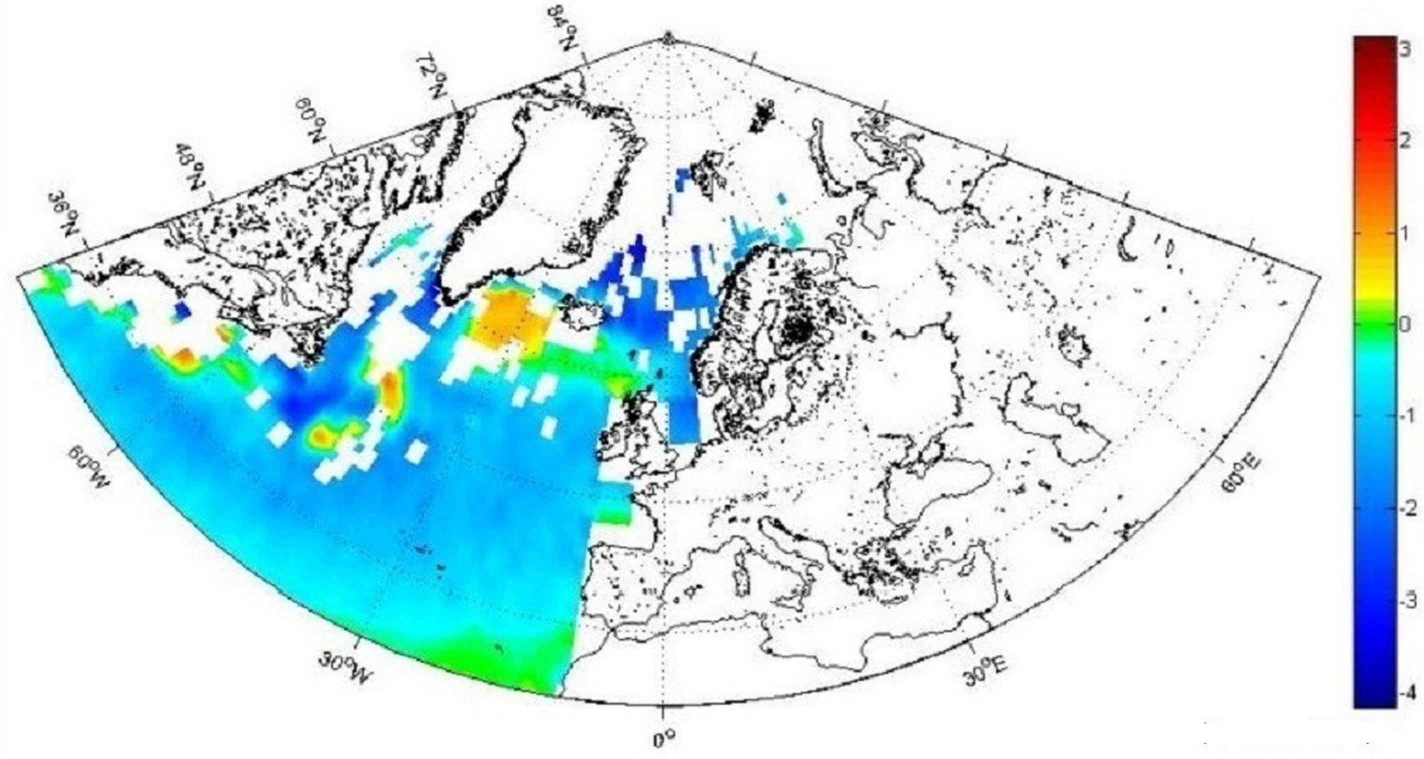

(mg C m^{-2} day^{-1})

b)

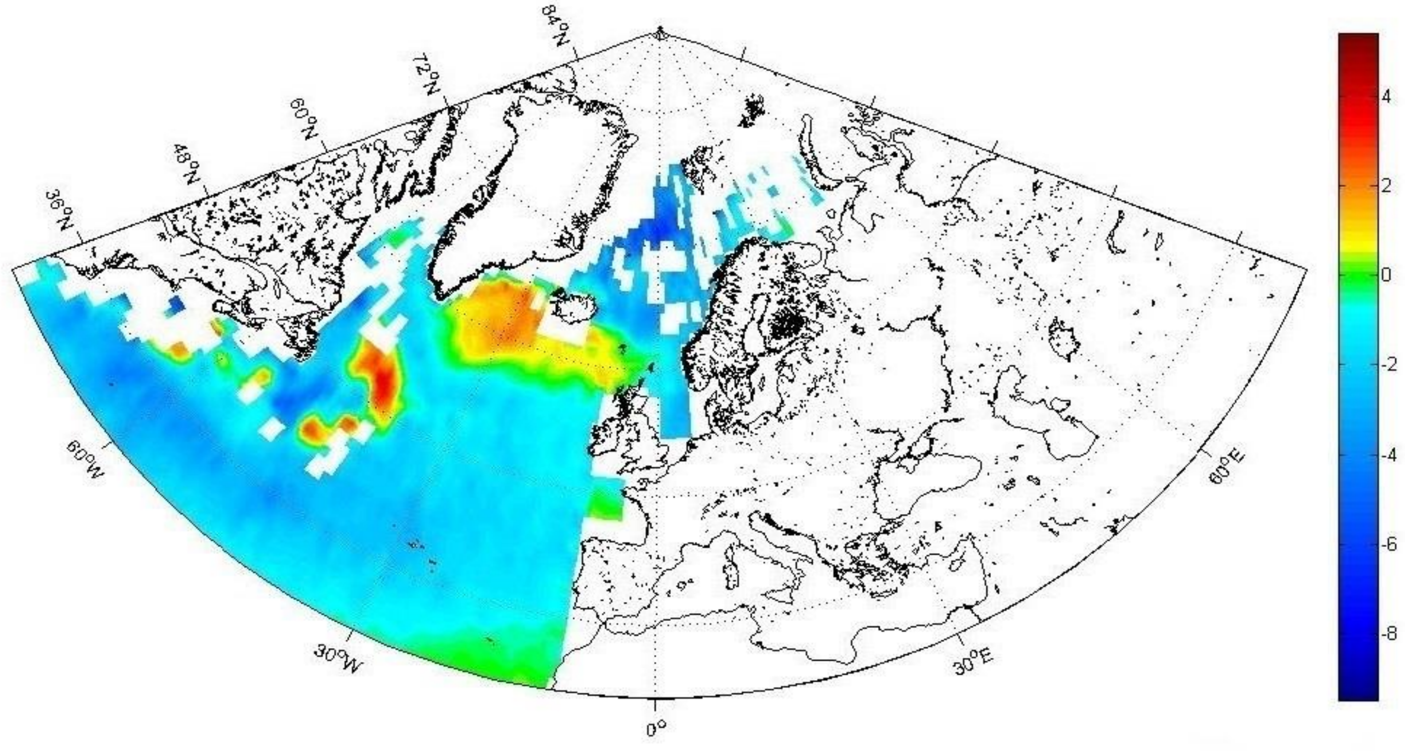

(mg C m^{-2} day^{-1})

c)

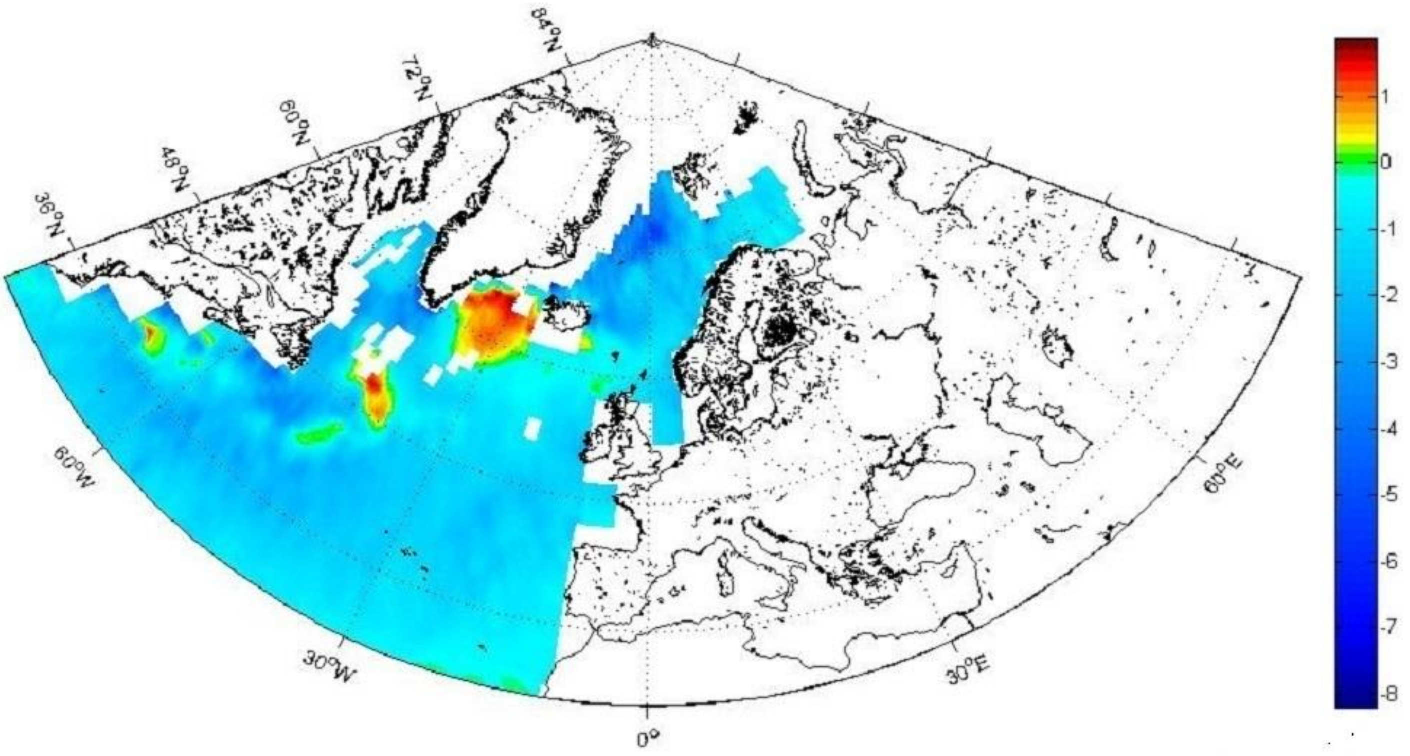

(mg C m^{-2} day^{-1})

d)

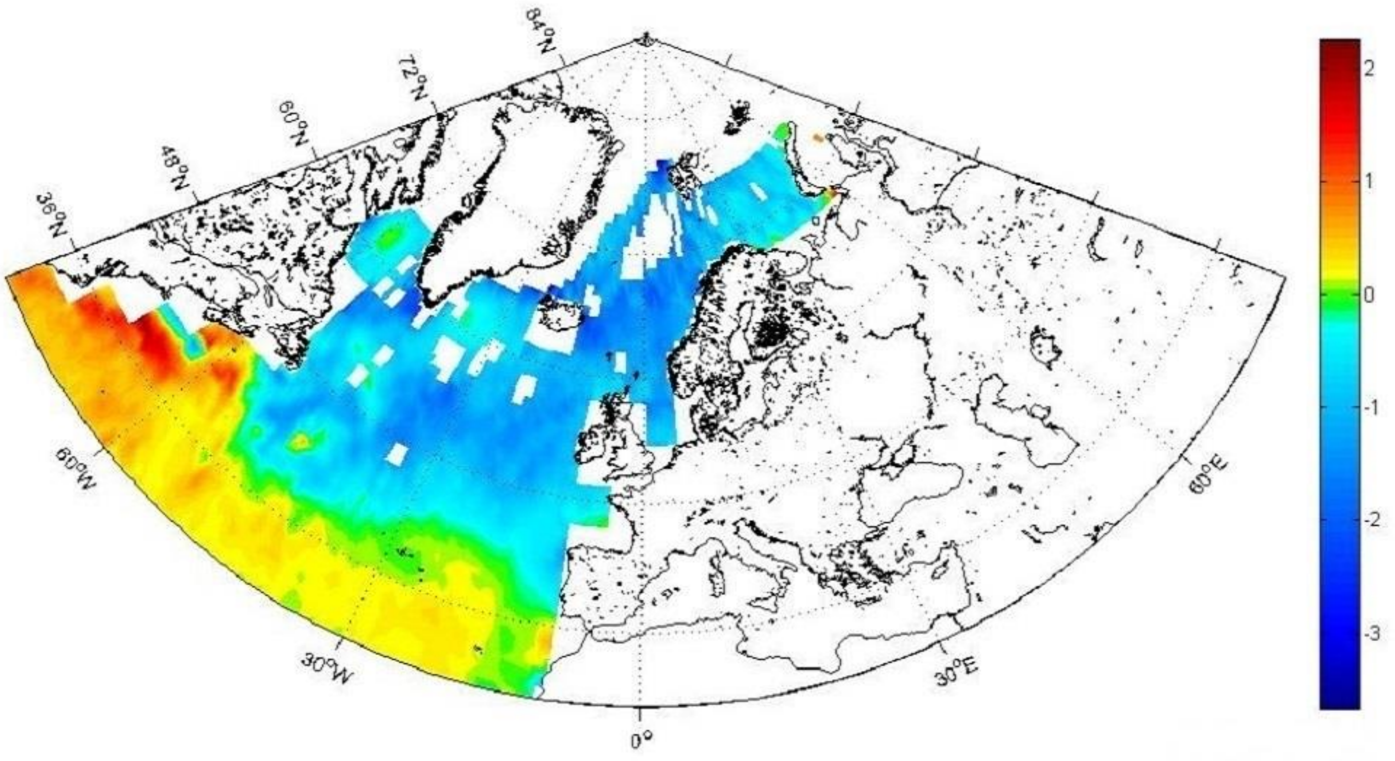

(mg C m^{-2} day^{-1})

e)

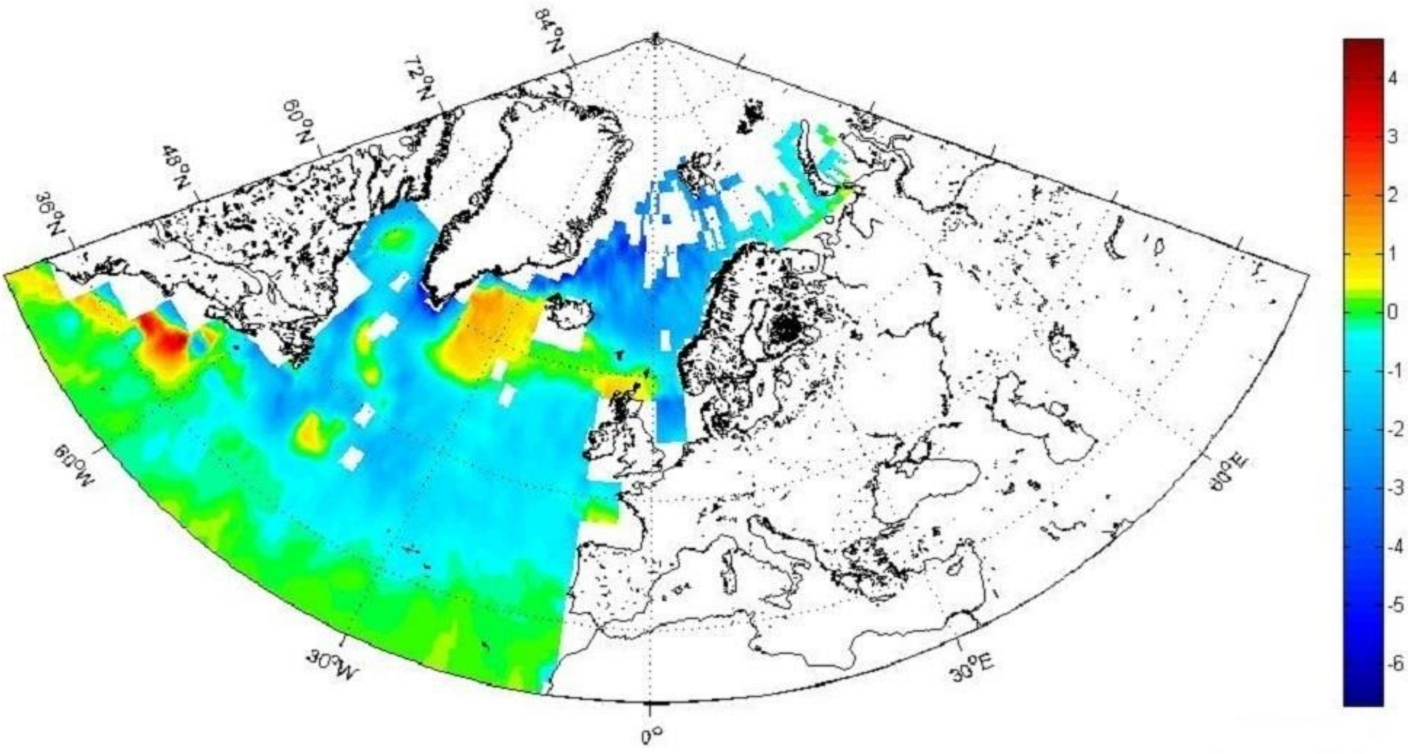

(mg C m^{-2} day^{-1})

Figure 4. Differences maps for the air-sea CO_2 fluxes (mg C m^{-2} day^{-1}) in the North Atlantic, between a wind cubed and squared parameterizations (Wanninkhof and McGillis 1999 and Wanninkhof 2014) in a) annual, b) DJF (Winter), c) MAM (Spring), d) JJA (Summer), e) SON (Autumn). The gaps (white areas) are due to missing data, land and ice masks..

a)

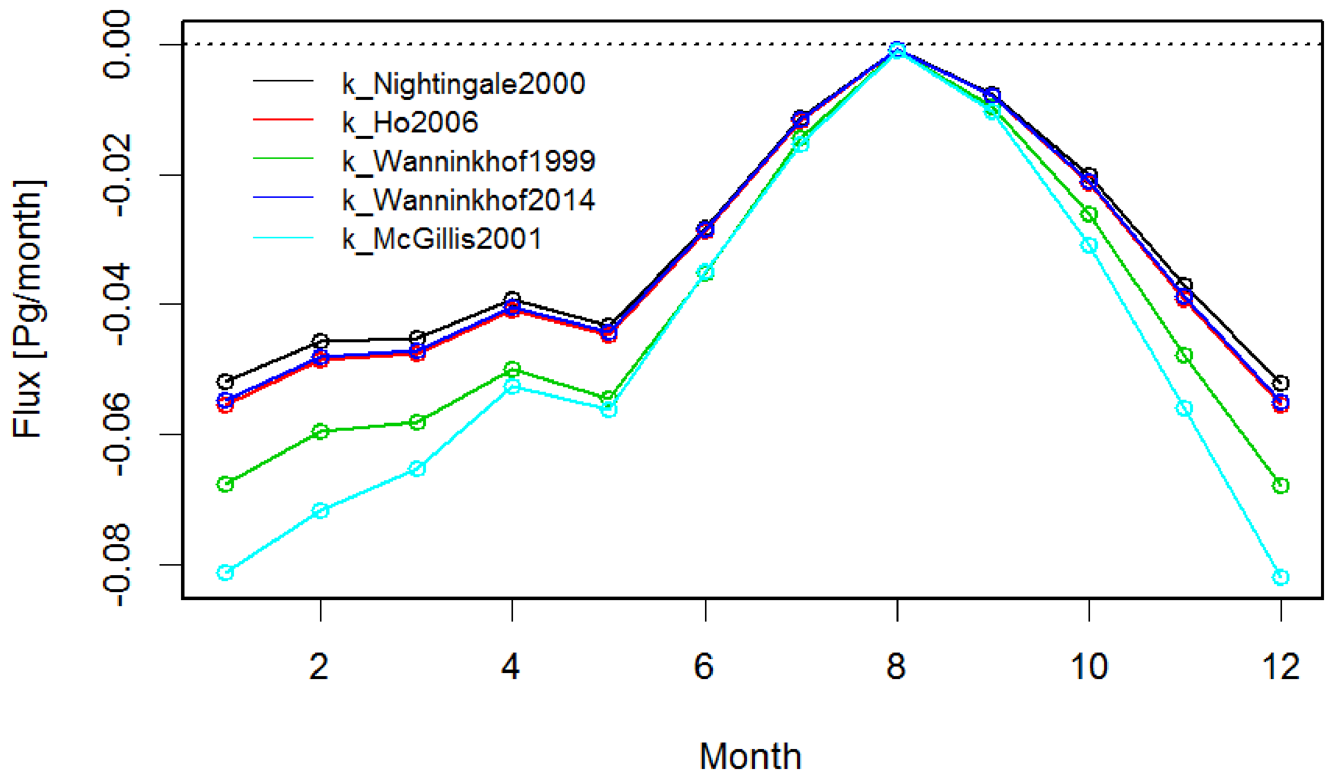

b)

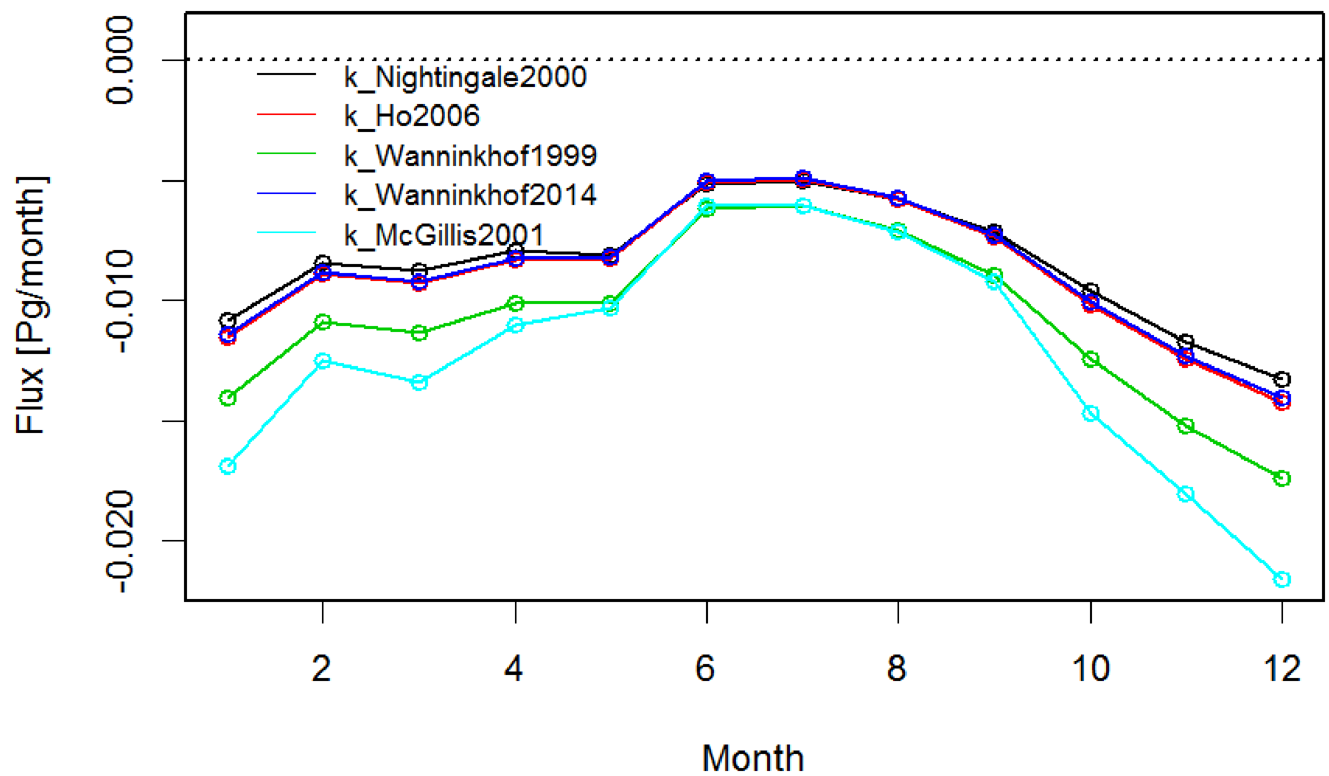

Figure 5. Monthly values air-sea fluxes of CO_2 (Pg/month) for the five parameterizations (eq. 4-8) in a) North Atlantic, b) European Arctic.

a)

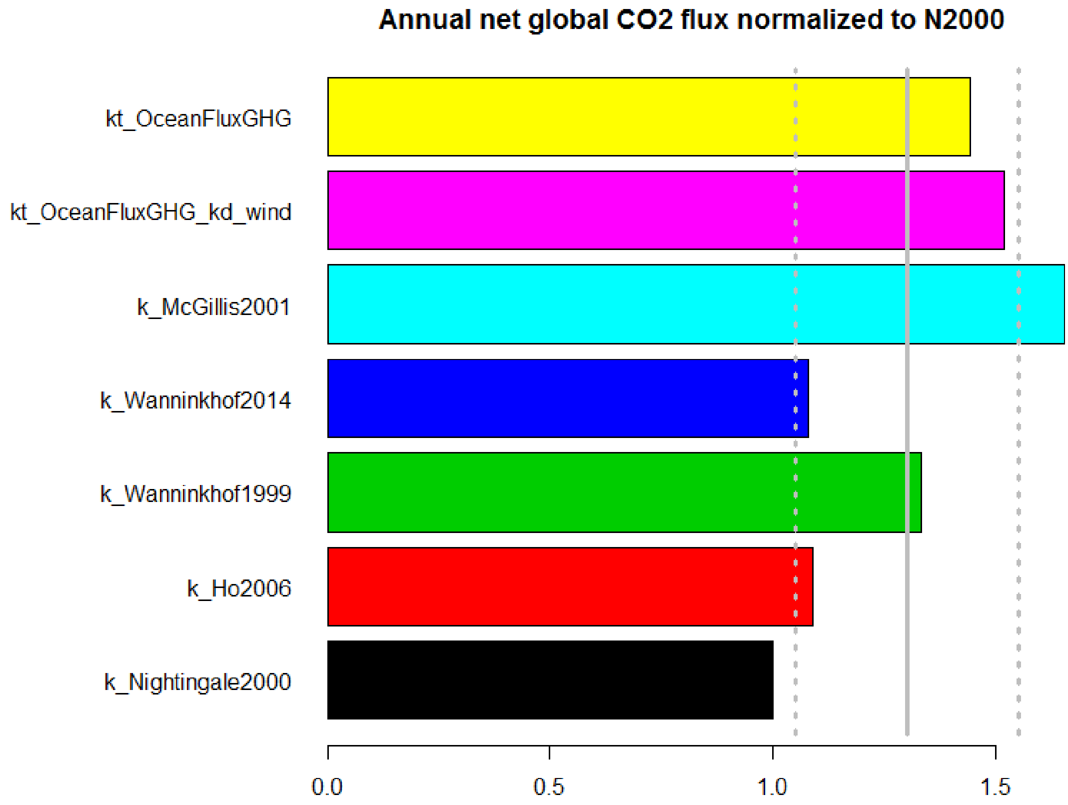
Annual net global CO2 flux normalized to N2000
kt_OceanFluxGHG
kt_OceanFluxGHG_kd_wind
k_McGillis2001
k_Wanninkhof2014
k_Wanninkhof1999
k_Ho2006
k_Nightingale2000
0.0
0.5
1.0
1.5

b)

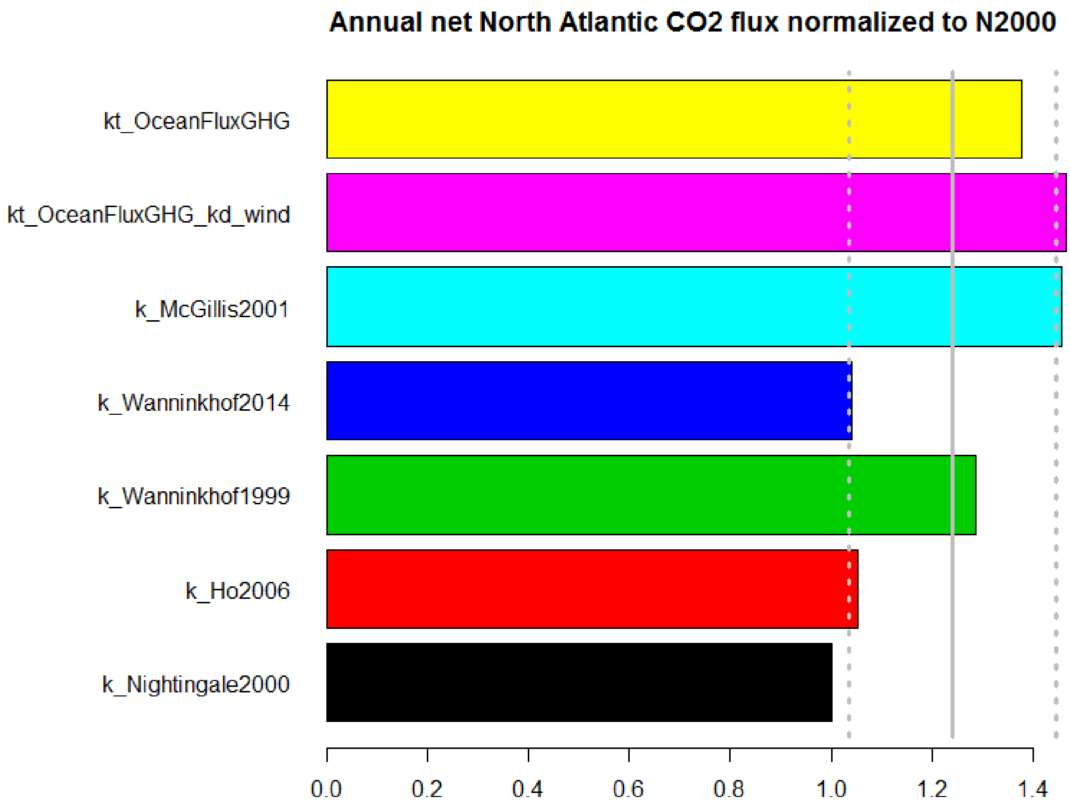
Annual net North Atlantic CO2 flux normalized to N2000
kt_OceanFluxGHG
kt_OceanFluxGHG_kd_wind
k_McGillis2001
k_Wanninkhof2014
k_Wanninkhof1999
k_Ho2006
k_Nightingale2000
0.0
0.2
0.4
0.6
0.8
1.0
1.2
1.4

c)

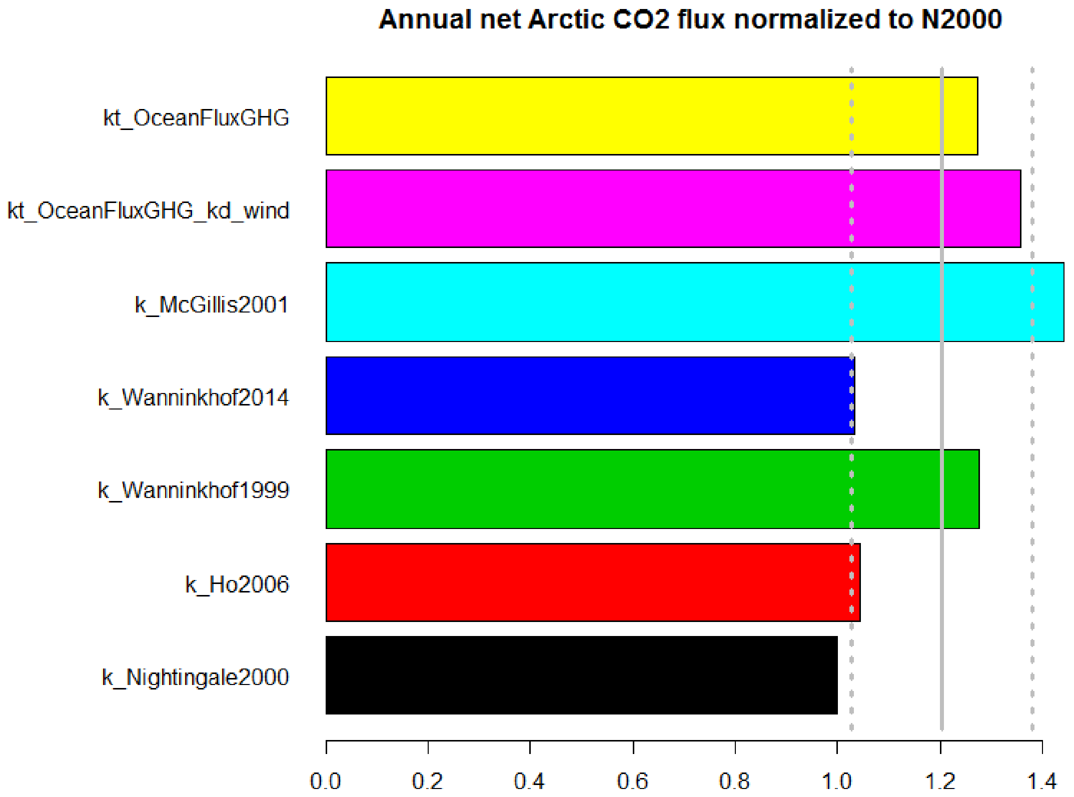

d)

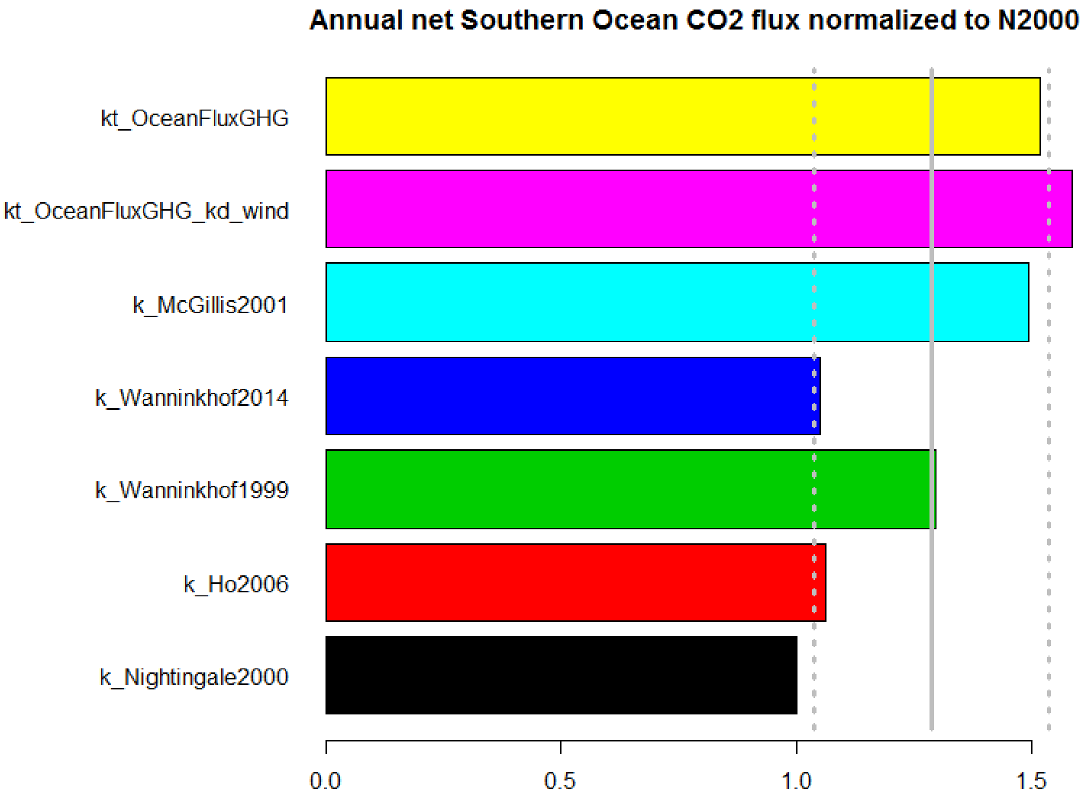

Figure 6. Annual air-sea fluxes of CO_2 for the five (eq. 4-8) parameterizations as well as for backscatter (default) and wind driven OceanFluxGHG parameterization normalized to flux values of Nightingale et al. (2000) *k* parameterization.

a)

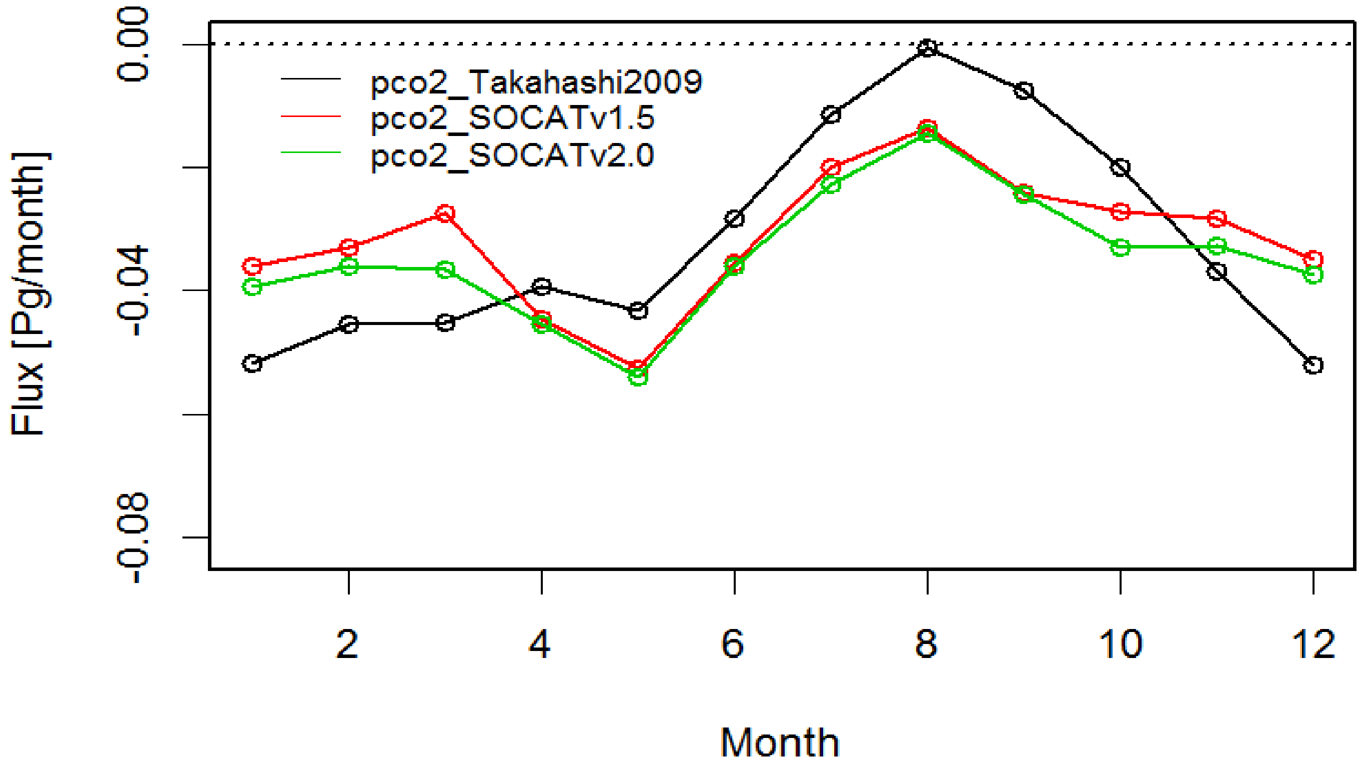

b)

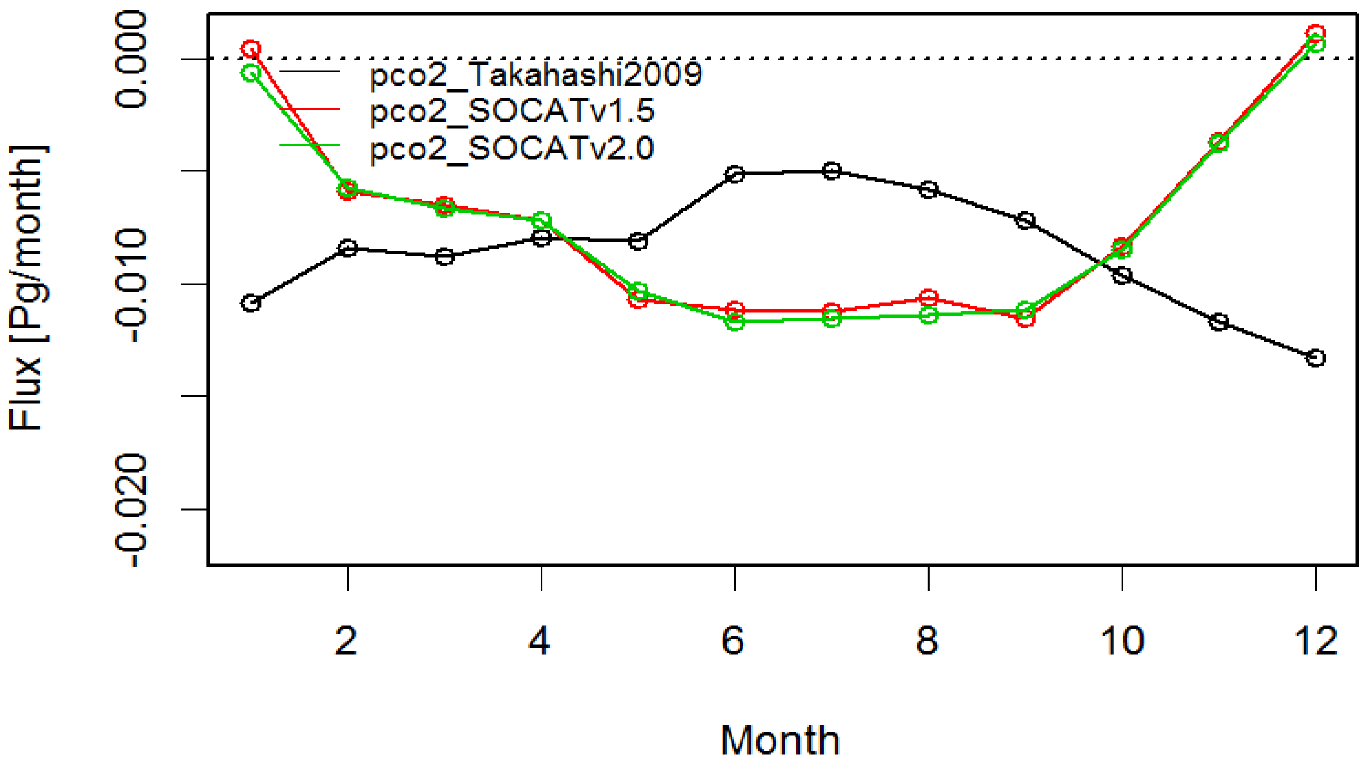

Figure 7. Comparison of monthly values fluxes of air-sea CO_2 fluxes calculated with different pCO_2 datasets (Takahashi et al., 2009, SOCAT v. 1.5 and 2.0) using the same *k* parameterization (Nightingale et al., 2000) in a) North Atlantic, b) European Arctic.

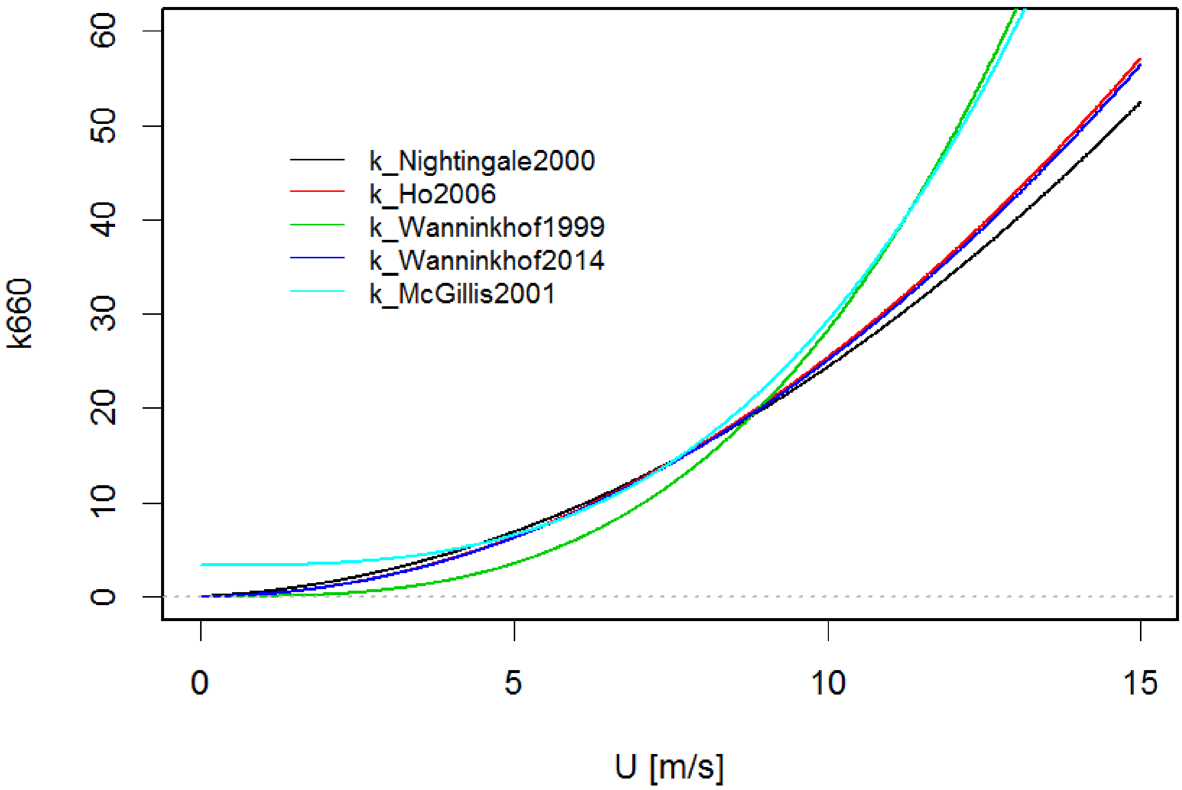

Figure 8. Different k660 parameterizations as a function of wind speed.